1   **Full title: Inferring causal pathways among three or more variables from steady-state**

2   **correlations in a homeostatic system**

3   **Short title: Inferring causality from steady-state correlations**

4

5   **Suraj Chawala[1]**

6   **Anagha Pund[1]**

7   **Vibishan B. [1]**

8   **Shubhankar Kulkarni[1]**

9   **Manawa Diwekar-Joshi[1]**

10   **Milind Watve[1]***

11   **[1]Biology, Indian Institute of Science Education and Research; Dr. Homi Bhabha Road,**

12   **Pashan, Pune, Maharashtra 411008, India**

13   ***for correspondence: milind@iiserpune.ac.in**

1

Abstract

Cross-sectional correlations between two variables have limited implications for causality. We show here that in a homeostatic system with three or more inter-correlated variables, it is possible to make causal inferences from steady-state data. Every putative pathway between three variables makes a set of differential predictions that can be tested with steady state data. For example, among 3 variables, A, B and C, the coefficient of determination, r_{AC}^2 is predicted by the product of r_{AB}^2 and r_{BC}^2 for some pathways, but not for others. Residuals from a regression line are independent of residuals from another regression for some pathways, but positively or negatively correlated for certain other pathways. Different pathways therefore have different prediction signatures, which can be used to accept or reject plausible pathways. We apply these principles to test the classical pathway leading to a hyperinsulinemic normoglycemic insulin-resistant, or pre-diabetic state using four different sets of epidemiological data. Currently, a set of indices called HOMA-IR and HOMA-β are used to represent insulin resistance and glucose-stimulated insulin response by β cells respectively. Our analysis shows that if we assume the HOMA indices to be faithful indicators, the classical pathway must in turn, be rejected. Among the populations sampled, the classical pathway and faithfulness of the HOMA indices cannot be simultaneously true. The principles and tools described here can find wide application in inferring plausible regulatory mechanisms in homeostatic systems based on epidemiological data.

2

Introduction

In the field of biomedicine, the nature of causality, and the use of correlations as an evidence for causality are much debated (1–6). There have been many attempts to develop sound methods to address questions of causal inference from correlational data which include Hill criteria (7), path analysis (8–11) the use of instrumental variables (12), Granger causality (13), Rubin causal model (14), or additive noise models (15). Hill criteria are a set of common sense criteria useful to avoid making misguided inferences. Path analysis generally assumes a direction of causality, and is useful in determining the contributions of different causal pathways to a process or a resultant variable. It generally assumes directed acyclic paths and its application to pathways with loops and cycles is difficult. Methods like Granger causality depend upon the assumption that the cause always precedes effect and that the variables show some degree of chaos or turbulence, so that there are notable events like sudden peaks in the variables, which can be tracked using longitudinal data. In evolved systems in which predictive adaptive responses are possible, the assumption that cause always precedes effect is questionable. Another class of methods like Propensity Score matching based on the Rubin causal model works well to estimate the effect of a causal factor, but does not take into account unobserved factors. The Rubin Causal Model also incorporates the structural equations model as it includes non-parametric forms as well (16,17). Models like additive noise can suggest the direction of the arrow of causality between two variables, but they require the assumption that either A causes B, or B causes A, without any confounding, looping or circularity (18,19).

More specifically, here we look at homeostatic systems which are extremely common in fields such as physiology. Homeostatic systems have a unique problem for causal inferences. Causal

59   inference can be based on time-series analysis with longitudinal data (19,20). Longitudinal

60   data are of little use however, if the time taken to reach equilibrium is smaller than the

61   observational window, or if the system is already in a steady-state. Most homeostatic systems

62   have negative feedback or some loop structures, because of which methods assuming acyclic

63   causal paths or freedom from confounding are not applicable.

64   Although the use of correlations to infer causality is doubted, intervention experiments are

65   generally taken as a convincing evidence of causality. However, causality in steady-state can

66   be substantially different than causality in a perturbed-state and inferences from a perturbation

67   experiment may not be applicable to steady-state causality. This necessitates a set of tools to

68   infer causality in a steady state which is independent of perturbing interventions. We argue in

69   this paper that it is possible to infer causal relationships among three or more variables from

70   cross-sectional data in a homeostatic system in which the variables and their relationships are

71   stable in time.

Motivation

Our motivation and the need for this tool came from some debated causal pathways in the pathophysiology of type 2 diabetes (T2D). According to the classical view, obesity-induced insulin resistance is primary, and rise in insulin levels is a compensatory response to insulin resistance, mediated by raised levels of glucose (21,22). This is contested (23), with increasing evidence suggesting that hyperinsulinemia precedes insulin resistance (24–28).Therefore the causal pathways between insulin levels, insulin resistance and plasma glucose are uncertain. There is also evidence of neuronal signals affecting insulin production on the one hand, and controlling glucose production by the liver partly independent of insulin on the other. Therefore, the causal relationship between insulin resistance, hyperinsulinemia and hyperglycemia needs to be re-examined (reviewed by (23)).

Elucidation of the causal pathway for a pre-diabetic or diabetic state is critical at the clinical level because the current approaches to medication are designed assuming one pathway but have largely failed to cure diabetes. If it is possible to determine causality reliably, it can potentially change diabetes medicine. It has long been recognized that levels of glucose and insulin are under homeostatic control, and that fasting is a steady state (29–32). With substantial data available on fasting levels of glucose and insulin from different populations, along with many other variables, a tool for inferring causality from a set of inter-correlated steady-state variables would help understand, and thereby better control T2D.

Beyond the specific problem of causality in pre-diabetes, a set of methods that can infer causality from steady-state data will find a large number of applications, not only in physiology and disease, but in many other areas of science. Although our investigations began

94   with the pathophysiology of diabetes, the emerging principles are generalizable and valuable

95   for inferential statistics in general.

Methods

We show here that when three inter-correlated variables are considered together with two or more causal arrows connecting them to make a causal pathway, each of the possible pathways makes a set of differential predictions by which the pathways can be differentiated from each other. Our approach to develop a method of inferring causality from cross sectional regression correlation parameters comprises following steps.

1. We first list the perceived possible hypothetical causal pathways among three variables.

2. For each pathway, we write a set of causal equations arising out of the hypothetical pathways. Steady-state solutions of these equations lead to a set of four general, and a few pathway-specific predictions. Each pathway therefore has a unique combination of such predictions or a prediction signature by which it can be differentiated from other pathways.

3. We test, using simulated data generated from assumed causal pathways, the conditions under which the predictions can be used to accept or reject a pathway reliably.

4. Based on these results, we suggest ways of handling multivariate data and infer causal networks among them.

5. We apply this logic to the specific case of pre-diabetes to examine the pathway classically thought to give rise to this condition.

Baseline assumptions and nomenclature

117   We consider three variables labelled A, B and C. Additional variables if needed to describe a

118   pathway will be labelled X, Y and so on. All causal relationships represented by a single

119   arrow are assumed to be linear, and all primary input variables are assumed to be normally

120   distributed. In a given operation, the slopes of causal pathways are assumed to be constant; the

121   errors in causal pathways are assumed to be distributed normally, with a mean zero and a

122   constant standard deviation, and no covariance with each other. We assume that the errors are

123   caused by variation in individual responses, and that a given individual's response is

124   consistent in time sufficiently long to reach a steady state. So the errors are randomized over

125   the population, but for a given individual, they are constant in time. We assume no

126   measurement errors in the baseline models. Since all our predictions are related to correlation

127   coefficients and regression slopes, we will ignore the intercepts for the sake of simplicity in

128   deriving many of the predictions.

129

The possible pathways

131   A variety of cyclic and acyclic pathways can exist in three variables. Fig 1 shows the simple

132   primary pathways that can exist. More can certainly be constructed by combinations of the

133   primary pathways. It is also possible to consider permutations of the three variables. For

134   example, the linear pathway among three variables can itself be written in six different ways.

135   Here we restrict to the primary pathways assuming a fixed sequence of the three variables

136   denoted by A, B and C. The principles that we derive from this set of primary pathways can

137   be extended to more complex pathways.

138

8

139   **Fig 1. Possible primary causal pathways between three variables.** More complex pathways

140   can be visualized by combinations of the primary ones.

141

Causal equations versus regression equations

143   Based on hypothesized pathways, we can write specific causal equations for each. The causal

144   equations are derived from the hypothesized pathway, while the regression equations can be

145   obtained from the given cross-sectional data using regression and correlation analysis. Our

146   causal equations are similar to the structural equations of (17). However, they differ in their

147   interpretation and treatment. In structural equations, the left hand terms are effects and right

148   hand terms are causes, and the two cannot be algebraically transferred without changing

149   causal interpretations. In our approach, after finding equilibrium solutions, we can carry out

150   algebraic operations freely in order to obtain testable predictions. The parameters of the

151   regression equation are not necessarily identical to those of the causal equations (Table 1). For

152   example, for a hypothesized pathway $Y = mX + C$, m is the causal slope, while the regression

153   slope would be underestimated if there is post-effect variability in X (33). Such a bias in the

154   slope is important in making and testing predictions. In the following section, we show that

155   the parameters of causal equations hold pathway-specific relationships with the parameters of

156   regression equations based on which, pathway-specific predictions about the regression

157   correlation parameters can be made.

158

159

9

160 **Table 1. List of abbreviations used.**

Abbreviation	Term	Remarks
A, B, C	Test variables	We have access from data
X, Y	Unknown variables	Which affect test variables. We do not have access to these from data.
M_{ij}	Slopes of regression of i on j	e.g. M_{ba} is calculated as $M_{ba} = \frac{cov(B,A)}{var(A)}$
K_{ij}	Intercept of regression of i on j	e.g. K_{ba} is calculated as $K_{ba} = \acute{B} - M_{ba}\acute{A}$
E_{ij}	Residuals of regression of i on j	e.g. E_{ba} is calculated as $E_{ba} = B - M_{ba}A - K_{ba}$
$m_1 m_2 m_3$	Slopes in causal equations	We do not have access to these in data
$e_1 e_2 e_3$	Error distribution in causal equations, assumed normal with mean zero and standard deviations sde_1 etc.	These are post-effect errors of the causal relationships which may get incorporated in pre-effect errors of a subsequent effect
$e_a e_b e_c$	Net variability in A, B and C	e.g. e_a is calculated as $e_a = A - \acute{A}$
$k_1 k_2$	Intercepts in causal equations	
$d_1 d_2$	Degradation /destruction rate constants in causal equations	Especially necessary to use in case of cyclic pathways

161

162   Table 1 legend: Parameters of causal equations are denoted by small letters and those of

163   regression equations by capital letters.

164

10

165   For ensuring steady-state, we assume that a given variable has a rate of formation/increase and

166   a rate of degradation/decrease. If the rate of degradation is positively dependent, or the rate of

167   formation negatively dependent on the standing level, then the variable invariably reaches a

168   steady state determined by the set of input parameters. Such steady states are characteristic of

169   homeostatic systems, and this principle is central to our methods.

170

171   For example, in a linear pathway $A \quad B \quad C$, $\frac{dB}{dt} = m'_1 A - d_1 B$ and $\frac{dC}{dt} = m'_2 B - d_2 C$. At a

172   steady-state the net change in any variable is zero. Therefore, the steady-state levels of B and

173   C will be $B = \frac{m'_1}{d_1} A = m_1 A$ and $C = \frac{m'_2}{d_2} B = m_2 B$ respectively.

174   In simple cases, we need not explicitly include the rates of degradation in the equations but

175   directly use parameters m_1 and m_2. For pathways involving loops and feedbacks the

176   relationships between variables are more complex and for such cases we will explicitly use

177   the degradation constants in the causal equations for ensuring steady-states.

178

Making predictions from steady-state solutions

180   We make four general predictions across all pathways and then formulate a null hypothesis

181   for each. In addition, there are certain pathway specific predictions that will be discussed

182   along with the description of the corresponding pathway. The four general predictions are:

183   1. Whether r_{AC}^2 can be estimated from the product of r_{AB}^2 and r_{BC}^2.

184   2. Whether slope M_{ca} can be estimated from the product of the slopes M_{ba} and M_{cb}.

11

185   3. Whether the residuals of the regression of B on A (E_{ba}) are correlated with those of C on B

186   (E_{cb}): The errors or residuals in a regression are assumed to be random independent

187   errors. However, we will show below that if there are loops, convergent or confounding

188   elements in a pathway, E_{ba} and E_{cb} do not remain independent. Based on the nature of

189   dependence between E_{ba} and E_{cb}, presence of, and possible nature of the loops and

190   convergence can be inferred.

191   4. a. Whether correction for A improves or reduces the correlation of B with C, i.e. whether

192       $r^2_{E_{ba}C}$ is greater or lesser than r^2_{BC}.

193   b. Whether the extent to which $r^2_{E_{ba}C}$ is greater or lesser than r^2_{BC} can be predicted by r^2_{AB}.

194   We will now state how each of the pathways makes specific predictions. For detailed formal

195   proofs and derivations refer to S1 Text.

Making and testing analytical predictions

Acyclic pathways

Linear Pathway (P1)

199   The causal equations for a linear pathway are:

$$A = input = \acute{A} + e_a$$

$$B = m_1 A + e_1 + k_1$$

$$C = m_2 B + e_2 + k_2$$

200   Where e_a, e_1, e_2 are not correlated.

201   Regression parameters can be derived from the causal equations as follows. Since in

202   regression of B on A, the slope $= cov\ (A,\ B)/var\ A$,

$$M_{ba} = \frac{\sum e_a e_b}{\sum e_a^2} = \frac{\sum e_a(m_1 e_a + e_1)}{\sum e_a^2} = \frac{m_1 \sum e_a^2}{\sum e_a^2} = m_1$$

$$M_{cb} = \frac{\sum e_c e_b}{\sum e_b^2} = \frac{\sum (m_2 e_b + e_2)e_b}{\sum e_b^2} = \frac{m_2 \sum e_b^2}{\sum e_b^2} = m_2$$

$$M_{ca} = \frac{\sum e_c e_a}{\sum e_a^2} = \frac{\sum (m_2 m_1 e_a + m_2 e_1 + e_2)e_a}{\sum e_a^2} = \frac{m_2 m_1 \sum e_a^2}{\sum e_a^2} = m_2 m_1$$

$$E_{ba} = e_b - M_{ba}e_a = m_1 e_a + e_1 - m_1 e_a = e_1$$

$$E_{cb} = e_c - M_{cb}e_b = m_2 e_b + e_2 - m_2 e_b = e_2$$

$$E_{ca} = e_c - M_{ca}e_a = m_2 e_b + e_2 - m_2 m_1 e_a = m_2 e_1 + e_2$$

203   For linear equations, there is little difference between the causal equations and regression

204   equations (Table 2). The regression equations therefore become

$$B = M_{ba}A + E_{ba} + K_{ba} = m_1 A + e_1 + k_1$$

$$C = M_{CA}A + E_{CA} + K_{CA} = m_2 B + e_2 + k_2$$

13

$$C = M_{CA}A + E_{CA} + K_{CA} = m_1 m_2 A + (m_2 e_1 + e_2) + (m_2 k_1 + k_2)$$

205   Prediction R1: Based on the equations above and Table 2, it can be shown that

206    $r_{AC} - r_{AB}r_{BC} = 0$ (See S1 Text 'Linear pathway: Prediction R1: Proof 1' for formal proof).

207   Prediction R2: From Table 2, it is obvious that the slope M_{ca} can be predicted from the

208   product $M_{cb}M_{ba}$; $M_{ca} - M_{cb}M_{ba} = m_1 m_2 - m_2 m_1 = 0$.

209   Prediction R3: From Table 2, as there is no covariance between e_1 and e_2,

210    $r^2_{E_{ba}E_{cb}} = r^2_{e_1 e_2} = 0$

211   Prediction R4: For a linear pathway, it can be shown that

212   (a) $r_{BC} > r_{E_{ba}C}$ and further, (b) $\frac{r^2_{BC} - r^2_{E_{ba}C}}{r^2_{BC}} = r^2_{AB}$

213   **Table 2. Relationship between the causal and regression equations for linear pathway.**

Slopes	Errors
$M_{ba} = m_1$	$E_{ba} = e_1$
$M_{cb} = m_2$	$E_{cb} = e_2$
$M_{ca} = m_1.m_2$	$E_{ca} = m_2 e_1 + e_2$

214

Radiating pathway (P2)

216   The causal equations for this model would be

$$A = m_1 B + e_1 + k_1$$

$$B = input = \acute{B} + e_b$$

$$C = m_2 B + e_2 + k_2$$

217   Note that the relationship between causal parameters and regression parameters is

218   substantially different in this pathway than the linear pathway (Table 3). For example, the

219   causal slope is $\frac{1}{m_1}$, but there is an underestimation of the slope during regression which is

220   predicted exactly by r_{AB}^2.

221   However, this difference is not detectable from cross-sectional data alone. Therefore, the

222   standard four testable predictions of this pathway remain similar to the linear pathway. We

223   will describe later that differentiating between pathways P1 and P2 is possible using a

224   different strategy.

225   Prediction R1: From Table 3, it can be shown that $r_{AC} - r_{AB} \cdot r_{BC} = 0$.

226   Prediction R2: From Table 3; we see slope M_{ca} can be predicted from the product $M_{cb} M_{ba}$

227   Prediction R3: From Table 3, $\quad \text{cov}(e_1, e_2) = 0 \therefore r_{E_{ba}E_{cb}}^2 = r_{e_1 e_2}^2 = 0$

228   Prediction R4: As formally shown in S1 Text ('Radiating pathway: Prediction R4: Proof 2'),

229    $r_{E_{ba}C} < r_{BC}$ and $\frac{r_{BC}^2 - r_{E_{ba}C}^2}{r_{BC}^2} = r_{AB}^2$

230   **Table 3. Relationship between the causal and regression equations for radiating pathway**

Slopes	Errors
$M_{ba} = \frac{1}{m_1} r_{AB}^2$	$E_{ba} = e_b(1 - r_{AB}^2) - \frac{1}{m_1} r_{AB}^2 e_1$
$M_{cb} = m_2$	$E_{cb} = e_2$
$M_{ca} = \frac{m_2}{m_1} r_{AB}^2$	$E_{ca} = m_2 e_b(1 - r_{AB}^2) - \frac{m_2}{m_1} r_{AB}^2 e_1 + e_2$

231

232

Convergent pathway (P3)

234   The causal equations for this model would be

$$A = input = Á + e_a$$

15

235
$$B = m_1 A + m_2 C + e_1 + k_1$$

$$C = input = \acute{C} + e_c$$

236   where $e_a, e_1,$ and e_c are uncorrelated.

237   Regression parameters derived from the causal equations are given in Table 4.

238   There are two pathway specific predictions for the convergent pathway, shared only by the

239   different cause pathway. Firstly, we expect no correlation between A and C from this pathway,

240   unless there are additional external pathways linking the two. The other unique feature of this

241   pathway is that both A and C have independent causal influence on B. As a result, the effect of

242   A adds to the error in the correlation between B and C and similarly, the effect of C

243   contributes to the error in the correlation between A and B. As a result, $r_{AB}^2 + r_{BC}^2$ cannot be

244   greater than 1, as shown below:

$$r_{AB}^2 + r_{BC}^2 = \frac{m_1^2 \sum e_a^2}{\sum e_b^2} + \frac{m_2^2 \sum e_c^2}{\sum e_b^2} = \frac{m_1^2 \sum e_a^2 + m_2^2 \sum e_c^2}{\sum e_b^2}$$

245    $\sum e_b^2 = m_1^2 \sum e_a^2 + m_2^2 \sum e_c^2 + \sum e_1^2$, so

$$r_{AB}^2 + r_{BC}^2 < 1$$

246

247   This prediction is so robust that if $r_{AB}^2 + r_{BC}^2 > 1$, the convergent pathway can be rejected

248   right away. Since we assume A and C to be independent input variables we assume no

249   correlation between them. However, if they are correlated due to some cause other than this

250   pathway, only then $r_{AB}^2 + r_{BC}^2$ can be greater than 1.

251

252   Prediction R1: Unlike pathways P1 and P2, for the convergent pathway, it can be seen that

253    $r_{AC}^2 - r_{AB}^2 . r_{BC}^2 < 0.$

16

254   Prediction R2: Since the expected slope M_{ca} is zero, and both M_{ba} and M_{cb} are non-zero, their

255   product is not a predictor of M_{ca}.

256      $|M_{ca}| - |M_{cb}M_{ba}| < 0$ as $|M_{ca}| = 0$

257   Prediction R3**:** The correlation $r_{E_{ba}E_{cb}}$ is predicted to have the same sign as M_{cb}.

258   Prediction R4: It can be shown that (a) $r_{BC} < r_{E_{ba}C}$ and further, (b) $\dfrac{r^2_{E_{ba}C} - r^2_{BC}}{r^2_{E_{ba}C}} = r^2_{AB}$.

259   Because this expression differs from R4 (b) of the earlier pathways, we can use a more

260   generalized form for R4 (b) as $\dfrac{\left|r^2_{BC} - r^2_{E_{ba}C}\right|}{max\left(r^2_{BC}, r^2_{E_{ba}C}\right)} = r^2_{AB}$

261   **Table 4. Relationship between the causal and regression equations for Convergent**

262   **pathway**

Slopes	Errors
$M_{ba} = m_1$	$E_{ba} = e_1 + m_2 e_c$
$M_{cb} = \dfrac{1}{m_2}r^2_{BC}$	$E_{cb} = e_c(1 - r^2_{BC}) - \dfrac{1}{m_2}r^2_{BC}(m_1 e_a + e_1)$
$M_{ca} = 0$	$E_{ca} = e_c$

263

264

Common cause pathway (P4)

266   The causal equations for this model would be

$$X = input = \acute{X} + e_x$$

$$A = m_1 X + e_1 + k_1$$

$$B = m_2 X + e_2 + k_2$$

$$C = m_3 X + e_3 + k_3$$

17

267   where $e_x e_1 e_2 e_3$ are not correlated.

268   It needs to be noted that $e_1 e_2 e_3$ are important in defining this pathway. If e_2 is negligible the

269   pathway approximates to the radiating pathway with *B* being the mediator between *A* and *C*.

270   Similarly, at small e_1, *A* becomes the mediator and at small e_3, *C* becomes the mediator in a

271   radiating pathway. For the way we have defined our predictions, e_2 is the most important error

272   term in this pathway (Table 5).

273   One very special feature of this pathway is that qualitatively it is highly symmetric with

274   respect to all the three variables *A, B* and *C*. This means that any permutation of them does not

275   change the qualitative nature of any prediction. This can be used as a pathway specific

276   prediction and a distinct signature for this pathway.

277   Prediction R1: It can be shown that $r_{AC}^2 > r_{AB}^2 . r_{BC}^2$ for this pathway.

278   Prediction R2: $|M_{ca}| - M_{cb}M_{ba} \vee 0$

279   Prediction R3: The sign of the correlation $r_{E_{ba}E_{cb}}$ is decided by the signs of m_1 and m_2. When

280   both have the same signs $r_{E_{ba}E_{cb}} = -ve$ and when they have opposing signs $r_{E_{ba}E_{cb}} = +ve$. In

281   other words the correlation multiplied by the sign of M_{ca} is always negative.

282   Prediction R4: For this pathway (a) $r_{E_{ba}C} < r_{BC}$ and (b) $\dfrac{r_{BC}^2 - r_{E_{ba}C}^2}{r_{BC}^2} r_{AB}^2$

283   **Table 5. Relationship between the causal and regression equations for common cause**

284   **pathway**

Slopes	Errors
$M_{ba} = \dfrac{m_2}{m_1} r_{AX}^2$	$E_{ba} = m_2 e_x (1 - r_{AX}^2) + e_2 - r_{AX}^2 \dfrac{m_2}{m_1} e_1$
$M_{cb} = \dfrac{m_3}{m_2} r_{BX}^2$	$E_{cb} = m_3 e_x (1 - r_{BX}^2) + e_3 - r_{BX}^2 \dfrac{m_3}{m_2} e_2$

$M_{ca} = \dfrac{m_3}{m_1} r_{AX}^2$	$E_{ca} = m_3 e_x (1 - r_{AX}^2) + e_3 - r_{AX}^2 \dfrac{m_3}{m_1} e_1$

285

Single different cause pathway (P5a)

287   The causal equations for this model would be

$$X = input = \acute{X} + e_x$$

$$A = input = \acute{A} + e_a$$

$$B = m_1 A + m_2 X + e_1 + k_1$$

$$C = m_3 X + e_2 + k_2$$

288   where $e_x e_a e_1 e_2$ are not correlated. Regression parameters derived are in Table 6.

289   Two specific predictions of this pathway shared only by the convergent pathway (P3) are that

290      $r_{AC}^2 = 0$ and that $r_{AB}^2 + r_{BC}^2 < 1$.

291   Prediction R1: $r_{AC}^2 - r_{AB}^2 . r_{BC}^2 < 0$

292   Prediction R2: $|M_{ca}| < M_{cb} M_{ba}$ ∨

293   Prediction R3: The correlation $r_{E_{ba} E_{cb}}$ is predicted to have the same sign as M_{cb}.

294   Prediction R4: (a) $r_{BC} > r_{E_{ba} C}$ and further (b $\dfrac{|r_{BC}^2 - r_{E_{ba} C}^2|}{max(r_{BC}^2, r_{E_{ba} C}^2)} = r_{AB}^2$ is true.

295   **Table 6. Relationship between the causal and regression equations for Single Different**

296   **Cause pathway**

Slopes	Errors
$M_{ba} = m_1$	$E_{ba} = m_2 e_x + e_1$
$M_{cb} = \dfrac{m_3}{m_2} r_{BX}^2$	$E_{cb} = m_3 e_x + e_2 - m_3 r_{BX}^2 \left(\dfrac{m_1 e_a}{m_2} + e_x + \dfrac{e_1}{m_2} \right)$

$M_{ca} = 0$	$E_{ca} = m_3 e_x + e_2 - m_1 e_a$

297

Double different causes pathway (P5b)

299   The causal equations for this model would be

$$X = input = \acute{X} + e_x$$

$$Y = input = \acute{Y} + e_y$$

$$A = m_1 X + e_1 + k_1$$

$$B = m_2 X + m_3 Y + e_2 + k_2$$

$$C = m_3 Y + e_3 + k_3$$

300   where $e_x e_y e_1 e_2 e_3$ are not correlated. Regression parameters derived are in Table 7.

301   Two specific predictions of this pathway shared only by the convergent pathway (P3) are that

302      $r_{AC}^2 = 0$ and that $r_{AB}^2 + r_{BC}^2 < 1$.

303   Prediction R1: $r_{AC}^2 - r_{AB}^2 . r_{BC}^2 < 0$

304   Prediction R2: $|M_{ca}| < M_{cb} M_{ba}$ ⱽ

305   Prediction R3: The correlation $r_{E_{ba} E_{cb}}$ is predicted to have the same sign as M_{cb}.

306   Prediction R4: (a) $r_{BC} > r_{E_{ba} C}$ and further (b) $\frac{\left| r_{BC}^2 - r_{E_{ba} C}^2 \right|}{max \left(r_{BC}^2, r_{E_{ba} C}^2 \right)} = r_{AB}^2$ is true.

307   It can be seen that all predictions of pathways P5a and P5b are identical and henceforth we

308   will treat both of them in a single group as pathway P5.

309

20

310 **Table 7. Relationship between the causal and regression equations for Double Different**

311 **Cause pathway.**

Slopes	Errors
$M_{ba} = \dfrac{m_2}{m_1} r_{AX}^2$	$E_{ba} = m_2 e_x (1 - r_{AX}^2) + m_3 e_y + e_2 - \dfrac{m_2}{m_1} r_{AX}^2 e_1$
$M_{cb} = \dfrac{m_4}{m_3} r_{BY}^2$	$E_{cb} = m_4 e_y (1 - r_{BY}^2) + e_3 - \dfrac{m_4}{m_3} r_{BY}^2 (m_2 e_x + e_2)$
$M_{ca} = 0$	$E_{ca} = m_4 e_y + e_3$

312

Pathways with loops

314 In pathways with loops, since there is a cyclic dependence between the variables we begin

315 with differential equations with variable-specific constant rates of disintegration that assure

316 steady states. This set of equations is then used to derive equilibrium solutions.

317

Positive or negative feedback pathway (P6)

319 The causal equations for this model would be

$$A = input$$

$$\frac{dB}{dt} = m_1 A - d_1 B + e_1 + m_f C + k_1$$

$$\frac{dC}{dt} = m_2 B - d_2 C + e_2 + k_2$$

320 where $e_a e_1 e_2$ are not correlated, and d_1 and d_2 are positive. For a consistent definition of

321 feedback, we assume m_1 and m_2 to always be positive, and that the sign of m_f decides

322 whether it is a positive or negative feedback loop. Feedback loops depend crucially on the

21

323   relative strength of the forward versus backward causation. If the feedback term, i.e. the effect

324   of C on B is weak, it approximates to a linear pathway, and if the forward term i.e. effect of B

325   on C is weak, it approximates to a convergent pathway. Therefore the predictions of linear or

326   convergent pathways can be expected if the forward or feedback links respectively are weak.

327   Additionally however, the negative feedback pathway is associated with a problem of

328   definition. If the feedback effect of C on B is stronger than the effect of B on C, the signs of

329   the slope in the causal and regression equations could be opposite, implying that while m_2 is

330   positive, M_{cb} could become negative. This happens when

331    $M_{cb} = \frac{m_2}{d_2} + \frac{\sum e_1\, e_2}{\sum e_b^2} < 0$ i.e. $\left| m_f \frac{\sum e_2^2}{\sum e_b^2} \frac{1}{(d_1 d_2 - m_2 m_f)} \right| > \frac{m_2}{d_2}$

332   This results in a paradoxical transformation of a causally negative feedback into an apparent

333   positive feedback since the sign of the slope and that of the feedback effect is the same.

334   Further, when the negative feedback is much stronger than the forward effect, the predictions

335   of convergent pathway are more applicable than the predictions of negative feedback

336   pathway. At equilibrium where both $\frac{dB}{dt}$ and $\frac{dC}{dt} = 0$, the equilibrium concentrations of B and C

337   are given by

$$B = \frac{m_1 d_2}{(d_1 d_2 - m_2 m_f)} A + \frac{d_2 e_1 + m_f e_2}{d_1 d_2 - m_2 m_f} + \frac{m_f k_2 + k_1 d_2}{d_1 d_2 - m_2 m_f}$$

$$C = \frac{m_2}{d_2} B + \frac{e_2}{d_2} + \frac{k_2}{d_2}$$

338   For simplification we take $m_1' = \frac{m_1 d_2}{(d_1 d_2 - m_2 m_f)}$, $e_1' = \frac{d_2 e_1 + m_f e_2}{d_1 d_2 - m_2 m_f}$ and $k_1' = \frac{m_f k_2 + k_1 d_2}{d_1 d_2 - m_2 m_f}$

$$B = m_1' A + e_1' + k_1'$$

339   Similarly $m_2' = \frac{m_2}{d_2}$, $e_2' = \frac{e_2}{d_2}$ and $k_2' = \frac{k_2}{d_2}$

22

$$C = m_2'B + e_2' + k_2'$$

340   It should be noted that $e_1' = \frac{d_2 e_1 + m_f e_2}{d_1 d_2 - m_2 m_f}$ and $e_2' = \frac{e_2}{d_2}$ share e_2, and would therefore co-vary.

341   The sign of this covariance is decided by the sign of m_f, i.e. whether the feedback is

342   positive or negative.

343   Regression parameters can be derived from the above as in Table 8.

344   Prediction R1: When the feedback is negative $r_{AC}^2 > r_{AB}^2 . r_{BC}^2$

345   The reverse applies for positive feedbacks where $r_{AC}^2 < r_{AB}^2 . r_{BC}^2$

346   Prediction R2: In negative feedback $M_{ca} > M_{cb} M_{ba}$ and in positive feedback $|M_{ca}| <$

347    $M_{cb} M_{ba}$.

348   Prediction R3: The sign of this correlation will be decided by the sign of m_f which is

349   negative for negative feedback and positive for positive feedback.

350   Prediction R4: (a) It can be shown that for negative feedbacks $r_{E_{ba}C} < (r_{BC})$. For positive

351   feedback the prediction is more conditional. The inequality $r_{E_{ba}C} < (r_{BC})$ will be true

352   above a threshold r_{BC}. For smaller r_{BC} it is difficult to make a definite prediction. (b) for

353   negative feedback $\frac{r_{BC}^2 - r_{E_{ba}C}^2}{r_{BC}^2} > r_{AB}^2$ and for positive feedback $\frac{r_{BC}^2 - r_{E_{ba}C}^2}{r_{BC}^2} < r_{AB}^2$ is true above

354   a threshold r_{BC}.

355

356   **Table 8. Relationship between the causal and regression equations for Positive or**

357   **negative feedback pathway.**

Slopes	Errors
$M_{ba} = m_1 = \dfrac{m_1 d_2}{(d_1 d_2 - m_2 m_f)}$	$E_{ba} = e_1 = \dfrac{d_2 e_1 + m_f e_2}{d_1 d_2 - m_2 m_f}$
$M_{cb} = m_2 + \dfrac{\sum e_1\, e_2}{\sum e_b^2}$ $= \dfrac{m_2}{d_2} + \dfrac{\sum e_1\, e_2}{\sum e_b^2}$	$E_{cb} = e_2 - \dfrac{\sum e_1\, e_2}{\sum e_b^2} e_b$ $= \dfrac{e_2}{d_2} - \dfrac{cov\left(\dfrac{d_2 e_1 + m_f e_2}{d_1 d_2 - m_2 m_f}\right)\left(\dfrac{e_2}{d_2}\right)}{\sum e_b^2} e_b$
$M_{ca} = m_2\, m_1$ $= \dfrac{m_2}{d_2} \dfrac{m_1 d_2}{(d_1 d_2 - m_2 m_f)}$	$E_{ca} = m_2\, e_1 + e_2 = \dfrac{m_2}{d_2} \dfrac{d_2 e_1 + m_f e_2}{d_1 d_2 - m_2 m_f} + \dfrac{e_2}{d_2}$

358

Positive or negative feed-forward pathway (P7)

360   The causal equations for this model would be

$$A = input = \acute{A} + e_a$$

$$A = m_1 X + e_1 + k_1$$

$$\frac{dB}{dt} = m_1 A - d_1 B + e_1 + k_1$$

$$\frac{dC}{dt} = m_2 B + m_3 A - d_2 C + e_2 + k_2$$

361   where $e_a e_1 e_2$ are not correlated. At equilibrium

362    $B = \dfrac{m_1}{d_1} A + \dfrac{e_1}{d_1} + \dfrac{k_1}{d_1} = m_1\, A + e_1 + k_1$ taking $m_1 = \dfrac{m_1}{d_1}, e_1 = \dfrac{e_1}{d_1}$ and $, k_1 = \dfrac{k_1}{d_1}$

$$C = \frac{m_1 m_2 + d_1 m_f}{d_1 d_2} A + \left(\frac{m_2}{d_1 d_2} e_1 + \frac{1}{d_2} e_2\right)$$

24

$$C = \frac{m_1 m_2 + m_f d_1}{d_2 m_1} B - \frac{m_f}{m_1 d_2} e_1 + \frac{e_2}{d_2} + \frac{k_2}{d_2}$$

363   We will take $m_2 = \frac{m_1 m_2 + m_f d_1}{d_2 m_1} e_2 = \frac{-m_f}{m_1 d_2} e_1 + \frac{e_2}{d_2}$

364   Note that since e_1 decides both e_1 and e_2 , the covariance between e_1 and e_2 will be

365     $\frac{-m_f}{m_1 d_2} e_1$, which will be positive when m_f is negative i.e. for negative feed-forward, and

366   negative when m_f is positive i.e. positive feed-forward.

367   For simplifying the definition of feed-forward, we assume m_1 and m_2 to be positive, and the

368   sign of m_f decides whether the feed-forward is positive or negative; a negative feed-forward

369   pathway is once again associated with a problem of definition. If the feed-forward effect of A

370   on C is stronger than that through B, and if their signs are opposite, the signs of slope in the

371   causal and regression equations could be opposites. That is, if $m_f d_1 > m_1 m_2$ then M_{cb} can be

372   negative although the causal relationship between B and C is positive. This results in a

373   paradoxical transformation of a causally negative feed-forward pathway into an effectively

374   positive feed-forward pathway as the product $M_{ba} M_{cb}$ and M_{ca} both have the same sign.

375   Note that while all the expressions are the same as in feedback pathways (Table 9), the

376   differences lie in the meanings of $\sum e_1' e_2'$, m_2' etc.

377   Prediction R1: For positive feed-forward $r_{AC}^2 > r_{AB}^2 . r_{BC}^2$, and for negative feed-forward

378     $r_{AC}^2 < r_{AB}^2 . r_{BC}^2$, but under conditions in which the result mimics positive feedback, $r_{AC}^2 >$

379     $r_{AB}^2 . r_{BC}^2$. This is the condition when a causally negative feed-forward transforms into an

380   apparent positive feed-forward.

381   Prediction R2: When m_f is positive, $M_{cb}M_{ba} < M_{ca}$. In the case of negative feed-forward

382    $M_{cb}M_{ba} > M_{ca}$ but under conditions in which a negative feed-forward transforms into a

383   positive feed-forward, $M_{cb}M_{ba} < m_1\ m_2\ = M_{ca}$.

384   Prediction R3: For positive feed-forward, we expect a negative correlation, and for negative

385   feed-forward, a positive correlation. Therefore, for positive feed-forward, the correlation

386    $r_{E_{ba}E_{cb}}$ will have the opposite sign of that of M_{cb}. For a negative feed-forward pathway, under

387   conditions when it transforms into an effective positive feed-forward correlation, $r_{E_{ba}E_{cb}}$ will

388   have the opposite sign of that of M_{cb}.

389   Prediction R4: (a) In the case of positive feed-forward $r_{E_{ba}C} < r_{BC}$ and in the case of negative

390   feed-forward prediction is conditional. Under the conditions when a causally negative feed-

391   forward becomes apparently positive feed-forward, the prediction of positive feed-forward is

392   true. When a negative feed-forward is effective $r_{E_{ba}C} < r_{BC}$ will be true above a threshold r_{AB}.

393   (b) For positive feed-forward $\dfrac{r_{BC}^2 - r_{E_{ba}C}^2}{r_{BC}^2} > r_{AB}^2$. For negative feed-forward a universal

394   prediction cannot be made. When the effect is that of a positive feedback the prediction of

395   positive feedback is true, otherwise $\dfrac{r_{BC}^2 - r_{E_{ba}C}^2}{r_{BC}^2} < r_{AB}^2$.

396

397 **Table 9. Relationship between the causal and regression equations for Positive or**

398 **negative feed-forward pathway.**

Slopes	Errors
$M_{ba} = m_1 = \dfrac{m_1}{d_1}$	$E_{ba} = e_1 = \dfrac{e_1}{d_1}$
$M_{cb} = m_2 + \dfrac{\sum e_1\, e_2}{\sum e_b^2}$ $= \dfrac{m_1 m_2 + m_f d_1}{d_2 m_1} + \dfrac{\sum e_1\, e_2}{\sum e_b^2}$	$E_{cb} = e_2 - \dfrac{\sum e_1\, e_2}{\sum e_b^2} e_b$ $= \dfrac{-m_f}{m_1 d_2} e_1 + \dfrac{e_2}{d_2} - \dfrac{\sum e_1\, e_2}{\sum e_b^2} e_b$
$M_{ca} = m_2\, m_1 = \dfrac{m_1 m_2 + m_f d_1}{d_2 m_1} \cdot \dfrac{m_1}{d_1}$	$E_{ca} = m_2\, e_1 + e_2$ $= \dfrac{m_1 m_2 + m_f d_1}{d_2 m_1} \cdot \dfrac{e_1}{d_1} + \dfrac{-m_f}{m_1 d_2} e_1$ $+ \dfrac{e_2}{d_2}$

399

Testing the null hypotheses

401 Testing in real life data needs to be different for equality and inequality predictions. The

402 prediction can serve as the null model wherever equality is predicted, but needs to be treated

403 as an alternative hypothesis wherever inequality is predicted. For pathways that predict

404 equality, a two-tailed probability is used, and for pathways predicting one-way inequality, a

405 one tailed test is used. In the results of simulations reported below, the convention

406 consistently followed through Figs 2 and 3 is that if H_0 is true, it is indicated by green, while

407 H_1 being true is indicated by red and H_2 being true by yellow.

408   R1: H_0: $r_{AC}^2 = r_{AB}^2 \cdot r_{BC}^2$, H_1: $r_{AC}^2 < r_{AB}^2 \cdot r_{BC}^2$ and H_2: $r_{AC}^2 > r_{AB}^2 \cdot r_{BC}^2$. Since every correlation

409   coefficient is associated with a confidence interval, to test the null hypothesis, we check that

410   the confidence interval of $r_{AC}^2 - r_{AB}^2 \cdot r_{BC}^2$ includes zero.

411   R2: H_0: $M_{ca} = M_{cb} M_{ba}$ (green), H_1: $M_{ca} < M_{cb} M_{ba}$ (red) and H_2: $M_{ca} > M_{cb} M_{ba}$ (yellow).

412   R3: Since the signs of causal slopes m_1 and m_2 are allowed to be positive or negative in the

413   models, the correlation coefficients are multiplied by the sign of the slope M_{cb}.

414   H_0: $r_{E_{ba}E_{cb}}^2 \cdot sign(M_{cb}) = 0$ (green), H_1: $r_{E_{ba}E_{cb}}^2 \cdot sign(M_{cb}) < 0$ (red) and H_2:

415    $r_{E_{ba}E_{cb}}^2 \cdot sign(M_{cb}) > 0$ (yellow).

416   R4a: H_0: $r_{BC}^2 = r_{E_{ba}C}^2$ (green), H_1: $r_{BC}^2 < r_{E_{ba}C}^2$ (red) and H_2: $r_{BC}^2 > r_{E_{ba}C}^2$ (yellow).

417   R4b: H_0: $\frac{\left| r_{BC}^2 - r_{E_{ba}C}^2 \right|}{max\left(r_{BC}^2, r_{E_{ba}C}^2 \right)} = r_{AB}^2$, H_1: $\frac{\left| r_{BC}^2 - r_{E_{ba}C}^2 \right|}{max\left(r_{BC}^2, r_{E_{ba}C}^2 \right)} < r_{AB}^2$, H_2: $\frac{\left| r_{BC}^2 - r_{E_{ba}C}^2 \right|}{max\left(r_{BC}^2, r_{E_{ba}C}^2 \right)} > r_{AB}^2$. Since the

418   prediction is about whether $\frac{\left| r_{BC}^2 - r_{E_{ba}C}^2 \right|}{max\left(r_{BC}^2, r_{E_{ba}C}^2 \right)}$ is predicted by r_{AB}^2, in the simulations results

419   reported below we show a scatter plot between the two where good predictions lie along the

420   diagonal and failure of prediction strays away from it.

421

422   **Fig 2. Analytical signatures for each pathway.** Summarizing the analytical signature for

423   each pathway in a color code where green represents acceptance of the null hypotheses H_0,

424   and red and yellow represent the acceptance of H_1 and H_2 respectively. Asterisks indicate

425   conditional prediction e.g.*r_{BC}^2 above a threshold, **r_{AB}^2 above a threshold.

426

427   **Fig 3. Simulation results of all pathways against all predictions.** For all acyclic pathways

428   and predictions from R1 to R4a, the result of every simulation run is plotted as a point with

429   r_{AB}^2 and r_{BC}^2 on X and Y axes respectively. Green represents null hypothesis true, red for H_1

430   and yellow for H_2. The results match very well with the predictions in Fig 2. For converging

431   and different cause pathways, a pathway specific prediction is that the sum of the two

432   correlation coefficients never exceeds unity. This is also evident in the simulation results.

433   For feedback and feed-forward pathways predictions from R1 to R4a, the X axis is r_{BC} and Y

434   is $\dfrac{m_2 sde_1}{m_f sde_2}$ which reflects the relative strength of the feedback or feed-forward term as

435   compared to the forward relation between B and C. The feed effect is strong when the ratio is

436   close to zero and weak moving away from it. For negative feedback and feed-forward the Y

437   axis goes from -1 to 0 and for positive feedback and feed-forward from 0 to 1. With negative

438   feedback and feed-forward, there is an apparent conversion to positive feedback and feed-

439   forward respectively under a set of conditions. When this happens r_{BC} becomes negative and

440   the predictions of positive feedback and feed-forward respectively apply. It can also be seen

441   that when the ratio is close to zero, predictions of converging pathway hold true.

442   Predictions from R4b for all pathways are shown as scatter plots with $\dfrac{\left|r_{BC}^2 - r_{E_{ba}C}^2\right|}{max\left(r_{BC}^2, r_{E_{ba}C}^2\right)}$ and r_{AB}^2.

443   When they are predicted equal, most points lie along the diagonal. Wherever inequality is

444   predicted, they are on one side of the diagonal.

445   Rejection due to overfitting inequality: For all inequality predictions, overfitting is possible.

446   For example, if we expect that $r_{AC}^2 > r_{AB}^2 . r_{BC}^2$, it is also possible that r_{AC}^2 is too large than what

447   can be predicted by the pathway under consideration. It is possible to test this either

448   analytically using equations derived for the corresponding predictions (see S1 Text), or using

449   simulations only if the parameters of the causal equations are known. If parameter estimates

450   for the pathways are known from independent empirical sources, it should be possible to test

451 over-fitting inequality. We will illustrate this with real life data later in the section 'Testing

452 specific pathways and questions: The case of pre-diabetes.'

453

Simulations to test the sensitivity and robustness of predictions

456 We used simulations to test the sensitivity and reliability of the analytical predictions. The

457 simulations were run using the causal pathway equations for each of the pathways *P1* to *P7* to

458 generate data, assuming the errors to be distributed normally around a mean zero. Up to 10000

459 simulations are run, with each run using randomly drawn parameters and error standard

460 deviations from a given range (see S1 Text 'Simulations used for testing the sensitivity and

461 robustness of the predictions' for details). The error standard deviation ranges were selected

462 such that the coefficients of determination were well spread between zero and one. The

463 generated data were then used to test the predictions of the corresponding pathway.

464 Simulations used in this section are not based on real life data, and are mainly employed to

465 test the reliability of the predictions over a range of regression correlation coefficients.

466

Agreement between analytical predictions and simulation results

468 Figs 2 and 3 show that simulations generally follow the analytical predictions quite well, but

469 with certain limitations. Many of the predictions, particularly when H_1 and H_2 are expected to

470 be true, work well above threshold values of *r*. When either r_{AB}^2 or r_{BC}^2 or both are small, the

471 null hypothesis fails to get rejected. This threshold of sensitivity can be reduced by increasing

472 sample size (n) (Fig 4). In the case of cyclic pathways, many predictions are conditional as

473   described above, and that is clearly reflected in the simulations. The agreement between

474   predictions and simulation results is weaker for a few specific pathway-prediction

475   combinations, in the sense that they work in a narrow range of conditions. This was seen in

476   case of P5 (different cause) prediction from R4b, and P7 (negative feed-forward) prediction

477   from R2. The predictions become more reliable at higher n. This implies that we need to be

478   conservative in rejecting pathways in such pathway-prediction combinations, particularly

479   when the correlation coefficients are small. Further, wherever the predictions are themselves

480   the null models, its rejection will naturally become conservative at low correlations. However

481   for inequality predictions, where the null hypothesis is equality, failure of rejecting the null

482   hypothesis should not be taken as rejection of the prediction when correlations are weak.

483   When we take such a conservative approach, rejection of a prediction can be confidently taken

484   to mean rejection of a pathway.

485

486   **Fig 4: Effect of n on the reliability of prediction.** Note that the parameter area over which

487   the simulation results match the prediction increases with n.

488

489   It can be seen from Table 10 that each pathway makes a set of predictions by which some

490   pathways can be differentiated from others. However, some have an identical set of

491   predictions among the general predictions described so far. Table 10 shows that there are 6

492   different signatures among 9 primary pathways. Some of the predictions are conditional, and

493   therefore, it may not always be possible to differentiate between pathways. For example, some

494   predictions do not work for very small r^2 values, or if feedback is not distinguishable from

495   linear pathways unless the feedback arrow is sufficiently strong. Such limitations are common

496   to all statistical tools, and they need to be used and interpreted in light of the appropriate

497   context and conditions.

498   **Table 10. Summary of predictions of all pathways considered.**

Prediction/ Rule → Pathway ↓	R1	R2	R3	R4 a	R4 b	Pathway specific prediction
P1 linear	$r^2_{AC} - r^2_{AB} \cdot r^2_{BC} = 0$	$|Mca| = |Mba.Mcb|$	$r_{Eba,Ecb} = 0$	$r_{Ebc,C}/r_{BC} < 1$	$\dfrac{|r^2_{E_{ba}C} - r^2_{BC}|}{\max(r^2_{E_{ba}C}, r^2_{BC})} = r^2_{AB}$	
P2 radiating	$r^2_{AC} - r^2_{AB} \cdot r^2_{BC} = 0$	$|Mca| = |Mba.Mcb|$	$r_{Eba,Ecb} = 0$	$r_{Ebc,C}/r_{BC} < 1$	$\dfrac{|r^2_{E_{ba}C} - r^2_{BC}|}{\max(r^2_{E_{ba}C}, r^2_{BC})} = r^2_{AB}$	
P3 convergent	$r^2_{AC} - r^2_{AB} \cdot r^2_{BC} < 0$	$|Mca| < |Mba.Mcb|$	$r_{Eba,Ecb} > 0$	$r_{Ebc,C}/r_{BC} > 1$	$\dfrac{|r^2_{E_{ba}C} - r^2_{BC}|}{\max(r^2_{E_{ba}C}, r^2_{BC})} = r^2_{AB}$	$r_{AC}=0$, $r^2_{AB}+r^2_{BC}<1$
P4 common cause	$r^2_{AC} - r^2_{AB} \cdot r^2_{BC} > 0$	$|Mca| > |Mba.Mcb|$	$r_{Eba,Ecb} < 0$	$r_{Ebc,C}/r_{BC} < 1$	$\dfrac{|r^2_{E_{ba}C} - r^2_{BC}|}{\max(r^2_{E_{ba}C}, r^2_{BC})} >= r^2_{AB}$	Symmetry around A,B,C
P5 different cause	$r^2_{AC} - r^2_{AB} \cdot r^2_{BC} < 0$	$|Mca| < |Mba.Mcb|$	$r_{Eba,Ecb} > 0$	$r_{Ebc,C}/r_{BC} > 1$	$\dfrac{|r^2_{E_{ba}C} - r^2_{BC}|}{\max(r^2_{E_{ba}C}, r^2_{BC})} = r^2_{AB}$	$r_{AC}=0$ $r^2_{AB}+r^2_{BC}<1$
P6 feedback negative	$r^2_{AC} - r^2_{AB} \cdot r^2_{BC} > 0$	$|Mca| > |Mba.Mcb|$	$r_{Eba,Ecb} < 0$	$r_{Ebc,C}/r_{BC} < 1$	$\dfrac{|r^2_{E_{ba}C} - r^2_{BC}|}{\max(r^2_{E_{ba}C}, r^2_{BC})} >= r^2_{AB}$	

P6 feedback positive	$r^2_{AC} - r^2_{AB} \cdot r^2_{BC} < 0$	$|Mca| < |Mba.Mcb|$	$r_{Eba,Ecb} > 0$	$r_{Ebc,C}/r_{BC} < 1$	$\dfrac{\left|r^2_{E_{ba}C} - r^2_{BC}\right|}{\max\left(r^2_{E_{ba}C}, r^2_{BC}\right)} >= < r^2_{AB}$
P7 feed-forward negative	$r^2_{AC} - r^2_{AB} \cdot r^2_{BC} < 0$	$|Mca| < |Mba.Mcb|$	$r_{Eba,Ecb} > 0$	$r_{Ebc,C}/r_{BC} < 1$	$\dfrac{\left|r^2_{E_{ba}C} - r^2_{BC}\right|}{\max\left(r^2_{E_{ba}C}, r^2_{BC}\right)} <= r^2_{AB}$
P7 feed-forward positive	$r^2_{AC} - r^2_{AB} \cdot r^2_{BC} > 0$	$|Mca| > |Mba.Mcb|$	$r_{Eba,Ecb} < 0$	$r_{Ebc,C}/r_{BC} < 1$	$\dfrac{\left|r^2_{E_{ba}C} - r^2_{BC}\right|}{\max\left(r^2_{E_{ba}C}, r^2_{BC}\right)} >= r^2_{AB}$

499   Table 10 legend: Note that there are 6 distinct signatures among 9 pathways. Pathways with

500   identical predictions are shaded with the same colour. There is some redundancy between the

501   predictions. For example the results of R1, R2 and R3 are tightly correlated. We feel that the

502   redundancy serves to validate and reinforce the predictions. Also when there are complex

503   pathways arising through combinations of primary pathways, different predictions show

504   differential departures from the primary pathway predictions. Therefore all predictions are useful

505   in spite of some redundancy.

506

Sensitivity analysis

508   The predictions derived and tabulated above are based on the typical assumptions of mainstream

509   statistics that the input variables are distributed normally and that all causal links are linear.

510   However, it is important to ask how critical these assumptions are for the predictions to work. In

511   experimental biology, the input variable is often designed to have uniform intervals and is not

512   normally distributed. A moderate deviation from linearity is also common in physiological and

513   other biological systems. If the predictions are too sensitive to these assumptions, they may

514   prove to be of limited use in real-life. We used Monte-Carlo simulations to assess whether the

515   predictions work under moderate deviations from these assumptions. When the input variables

516   were selected randomly from a uniform rather than a Gaussian distribution, all predictions

517   worked with nearly the same differentiating ability (data not shown). Similarly, when non-

518   parametric Spearman ranked correlations were used instead of Pearson's correlations, the

519   correlation related predictions (from R1 and R4) worked similarly (data not shown). This

520   demonstrates that the tools are not too sensitive to the assumptions of normality of input variable,

521   linearity of relationships, and parametric or non-parametric nature of correlations.

Applications of the method

Accepting or rejecting pathways using real-life data

Two approaches are possible by which the predictions of a pathway can be tested using real-life data. (i) Based on confidence intervals of correlations and regression slopes: The null hypotheses for every prediction can be tested using calculation of confidence intervals of regression correlation parameters. Simulations have shown that except when the underlying correlation coefficients are too low, this approach can be reliably used to test the predictions. The sensitivity of predictions depends upon the sample size as well as the position in the parameter space (Fig 3). It is likely therefore that at smaller sample sizes, or at lower r_{AB}^2 or r_{BC}^2, pathways that predict H_1 or H_2 may fail to get support even if true. On the other hand, at lower r_{AB}^2 or r_{BC}^2 if a pathway predicts H_0 to be true and the null hypothesis gets rejected, the rejection can be highly reliable. (ii) Monte-Carlo simulation approach: An alternative approach, which will be more conservative in rejecting pathways, is the Monte-Carlo approach. Assuming a specific pathway to be true, it is possible to back calculate the causal equation parameters from the regression correlation parameters obtained in the data (Tables 2 to 9). For pathways such as negative or positive feedback, it is not possible to estimate all causal parameters from regression parameters. In such cases, if empirical estimates of one or a few causal parameters can be obtained, the remaining causal parameters can be worked back. Using the estimated parameters of causal equations, Monte-Carlo simulations can be run to obtain the probabilities of getting the observed results. This approach can be particularly useful when the correlations obtained in the data are weak, and a conservative inference is preferred.

Distinguishing between pathways with identical signatures

From the predictions summarized in Table 10, it can be seen that some pathways share prediction signatures. For example, the linear pathway cannot be distinguished from radiating or convergent, is indistinguishable from different cause. There are three possible ways of resolving between pathways with similar signatures: (i) Swapping variables: In the generalized predictions, common cause pathway and negative feedback pathway have the same predictions. However, the predictions of the common cause pathway are symmetric around A, B and C, and flipping the positions of the three variables does not alter the predictions, which is not the case with negative feedback pathway. (ii) Involving a fourth variable whose causal relationship with at least one of the triad is already known, or (iii) involving more variables to cross validate pathways. We will discuss (ii) and (iii) in a different context below.

Inferring causality between two variables

It is extremely difficult to infer causal relationship between two correlated variables. Although some solutions have been suggested, their applicability is limited (15, 16). However, it is possible to infer the causal relationship between two variables if we have data on a third variable that is correlated with one or both of them with known causality. For example, in men, testosterone levels and muscle strength are correlated, but the direction of the causal arrow might be uncertain since testosterone can increase muscle mass, while (34) exercise can also induce a testosterone response (35,36). The causal relationship can be revealed in cross-sectional data if we use chronological age as a third variable. Neither testosterone nor muscle mass decides the chronological age, but age may affect one or both the variables. If age shows significant correlation with one or both the variables, the predictions from different possible pathways can

37

567   be tested using the set of predictions as described. By testing these predictions, it should be

568   possible to determine the causal relationship between muscle mass and testosterone.

569

Inferring causal pathways with three variables

571   To infer causal pathways within three intercorrelated variables, three alternative approaches are

572   possible. The first approach is to test and resolve between preconceived hypothetical pathways.

573   It is likely that prior knowledge or some insights into mechanisms allow us to start with a few

574   plausible alternative pathways. It is possible to perceive more complex pathways by

575   combinations of the primary pathways that we considered in this paper. For example, a pathway

576   may contain both feedback and feed-forward elements. Such complex or combinational

577   pathways can be used to make a set of predictions by the analytical approach described above,

578   and testing these predictions can resolve between pathways. If we do not have such preconceived

579   pathways, it would be necessary to consider all possible combinations of pathways between the

580   three variables, and make differential predictions from each of them. In such cases, we must also

581   consider permutations of the variables. At the end, it may not be possible to ascertain a single

582   unique causal pathway since the prediction signatures of some of them may be identical.

583   Nevertheless, it would still be possible to reject some pathways based on their prediction

584   signature. In addition, if available, we can involve a fourth variable correlated to one or more of

585   the three, if there is some pre-existing knowledge about its causal relationship.

586

Inferring causal networks with more than three variables

588   In complex systems, often there are large causal networks. In such networks, combinations of 3

589   membered motifs can be identified. Out of the possible pathways among three variables some

590   can be rejected using analysis of the three variables. Bringing in a fourth one can provide

591   additional insights which can be used for cross checking or validating our first set of inferences.

592   In complex causal networks, there can be many such cross check and validation possibilities. For

593   large networks algorithms requiring massive computational power may be needed that may pin

594   down one or a few network structures from the large number of possible ones using

595   combinations of three member motifs and cross validation facility among the motifs.

596

Testing specific pathways and questions: The case of pre-diabetes

599   Apart from some common pathways described above, it is possible that real life problems have

600   some added complications due to which, the standard solution of testing a fixed set of predictions

601   may not be sufficient. However, one can apply similar foundational principles to handle such

602   pathway-specific questions. We will illustrate this using a classical hypothesis that attempts to

603   explain a human physiological state designated as an insulin resistant, hyperinsulinemic,

604   normoglycemic, pre-diabetic state. In this state, the plasma levels of fasting insulin (FI) are

605   raised although fasting glucose (FG) remains normal. The classical interpretation of this state

606   (Fig 5a) is that a rise in insulin resistance, presumably as a result of obesity, is primary. Insulin

607   resistance interferes with insulin-induced glucose uptake by muscle and other insulin-dependent

608   tissues. The reduced uptake raises plasma glucose levels. The raised plasma glucose induces

609   extra insulin secretion so that plasma insulin levels go up. The extra insulin compensates for

610   insulin resistance and normalizes glucose level. As a result, the fasting steady state of an insulin-

611   resistant individual is characterized by raised FI and normal FG. At steady state, insulin

612   resistance is measured by the index, HOMA-IR (defined as $\frac{Insulin(IU).Glucose\left(\frac{mg}{dL}\right)}{405}$), and the β

613   cell response to glucose, by the index, HOMA β (defined as $\frac{360.Insulin(IU)}{Glucose\left(\frac{mg}{dL}\right)-63}$). Both the indices are

614   based on the assumption of a steady state.

615

616   **Fig 5:** Possible pathways between insulin resistance, FG and FI: a) A simplified single feedback

617   pathway that approximates the negative feedback pathway P6. b) A null model assuming FG and

618   FI to be independent and HOMA-IR a derived construct. c) An improvised null model with an

619   external causal factor influencing FG and FI. d) The classically perceived pathway with dual

620   feedback from glucose and insulin.

621

622   A logical flaw in this interpretation is that, after the glucose levels return to normal, there is no

623   reason why FI should remain high. Insulin has a short half-life of about 6 minutes (32,37) and

624   therefore a steady state level can be achieved quite fast; 12 hour fasting should be sufficient to

625   achieve such a steady state. Therefore, a steady state in which FI is raised but FG remains normal

626   is not well explained by the classical theory. In spite of this flaw, the main stream thinking in this

627   field has held on to this interpretation for over four decades, and the indices HOMA-IR and

628   HOMA- β continue to be commonly used in epidemiological research. Challenges to this causal

629   interpretation come from the arguments and evidence that rise in FI precedes insulin resistance

630   (24–28,38). Therefore, there is a need to reexamine the classical causal pathway. We will test

631   this pathway based on our interpretations of the interrelationships of the regression-correlation

632   parameters.

633   The pathway in question is more complex than the basic set of pathways P1 to P7. For regulation

634   of glucose production by the liver and glucose uptake by tissues, there is a dual negative

635   feedback. One feedback is exerted by glucose itself, which enhances tissue uptake and

636   suppresses liver glucose production. The other feedback operates through insulin, which

637   facilitates glucose uptake by insulin-dependent tissues and suppresses liver glucose production.

638   If we ignore the direct glucose feedback and assume that feedback regulation operates only

639   through insulin, then there is a single negative feedback. Thus the pathway can be simplified to

640   the negative feedback pathway P6. If we incorporate dual feedback, as the equations show

641   below, the relationship between insulin resistance and FG is not strictly linear. We could

642   therefore use the standard set of predictions of a negative feedback model, assuming a single

643   feedback. Alternatively, we can use the dual feedback model, and apply simulations to make and

644   test predictions, since empirical estimates for most of the parameters are available from

645   experiments (see S2 Text).

646   However, the main problem in testing these pathways is that we have no direct measure of

647   insulin resistance. HOMA-IR and HOMA-β are believed to measure insulin resistance and β cell

648   response respectively, but they are derived from the other two variables, which makes the

649   problem tricky and circular. We approach the problem using more than one set of assumptions.

650   (i) First, we test the dual feedback pathway (Fig 5d) assuming HOMA-IR and HOMA-β to

651   faithfully represent insulin resistance and β cell response respectively. (ii) Then, we examine the

652   constraints laid down by deriving these two parameters from the other two variables. (iii) In

653   comparison, we use a null model (Fig 5b) in which the classical pathway is not true, there is no

654   relationship between FG and FI, and HOMA-IR and HOMA-β are artificial constructs derived

655   from the two measured variables and may not reflect any real phenomenon. We also test the

656   typical convergent model, in which FG and FI determine HOMA-IR. (iv) Using some

657   oversimplification, ignoring non-linearity of the model and assuming that HOMA-IR and

658   HOMA-β are faithful indicators, we test the classical predictions of the negative feedback

659   pathway (Fig 5a) as described earlier. We use epidemiological data on FG and FI measurements

660   in four populations to test the classical causal pathway using our approach.

661

Data sources

663   We used four data sets of sample studies by two research groups. All the four sets contain

664   individuals with and without overt type 2 diabetes. Since we are addressing the prediabetic state

665   here we have taken the non-diabetic subset of *n* individuals from the four samples. (i) Coronary

666   Risk of Insulin Sensitivity in Indian Subjects (CRISIS) Study, Pune, India (39) (n=558). (ii and

667   iii) Newcastle Heart Project (NHP), England, (40) which has data on populations of two different

668   ethnic origins namely European white (n=595) and south Asian (n=413). (iv) Pune Maternal

669   Nutrition Study (PMNS), Pune, India (41) (n=299). All the predictions are tested independently

670   in all the four data sets.

671

The dual feedback model (Fig 5d)

673   We assume that the standing plasma glucose level is a result of baseline rate of glucose

674   production by the liver; suppression of this production as well as muscle glucose pickup which is

675   proportional to the standing glucose level (direct glucose feedback); the insulin mediated

676   suppression as well as uptake (insulin mediated feedback) and individual variability. The

677   standing insulin levels are a result of glucose stimulated insulin secretion on the one hand and

678   insulin degradation on the other. Thus, the causal equations can be written as

679

$$\frac{dG}{dt} = L - K_1.G - I_{SENS}.K_2.I + e1$$

680

$$\frac{dI}{dt} = K_3.G - d.I + e_2$$

681

682   Where G and I are plasma levels of glucose and insulin respectively, and FG and FI are the

683   fasting steady state levels of the same. K_1 denotes the rate constant for negative feedback of

684   glucose on liver glucose production and tissue glucose uptake; K_2 denotes the rate constant for

685   insulin-mediated feedback which is proportional to I_{SENS}, the insulin sensitivity of tissues; K_3 is

686   the rate constant for glucose-induced insulin release; and $d,$ the rate of insulin degradation.

687

688   Steady state solution: By assuming the net change to be zero in a steady state, we get

$$FG = \frac{d(L + e_1) - I_{SENS}K_2 e_2}{dK_1 + I_{SENS}K_2 K_3}$$

$$FI = \frac{K_3 FG + e_2}{d}$$

689   It can be seen that the steady state glucose level is a function of insulin resistance (*IR*) which is a

690   reciprocal of insulin sensitivity. Using the reciprocal, we can write

691

$$FG = \frac{IR.d(L + e_1) - K_2 e_2}{IR.dK_1 + K_2 K_3}$$

692

693   Thus the relationship between FG and IR is non-linear and follows a saturation curve.

694   Testing the pathways by the four different approaches described above:

43

695 (i) Assuming classical pathway and faithful indices: The following predictions of the

696 classical pathway depicted in Fig 5d and modeled above are testable.

697 (a) HOMA-IR, FG and FI should be positively correlated to each other. This

698 prediction is true in all the four data sets except that the correlations between FG

699 and FI are weak in all the four data sets. In terms of the variance explained (range

700 2.6 to 4.9 %) FG and FI are poorly related (Table 11a). The glucose homeostasis

701 model expects a positive correlation between FG and FI. It is important to realize

702 this since in the classical thinking, a prediabetic state is characterized by increased

703 insulin but normal glucose levels. If the compensatory insulin response is mediated

704 through glucose, it is impossible to have a raised FI without a proportionate rise in

705 FG. In the pathway predictions, a positive correlation between FG and FI is

706 expected independent of the feedback loop. However the classical thinking tries to

707 explain a hyperinsulinemic normoglycemic state achieved through this pathway.

708 The poor correlation between FG and FI, and a large coefficient of variation in FI

709 compared to FG indicates that a normoglycemic hyperinsulinemic state may

710 indeed be achieved, but whether the classical pathway offers a sound explanation

711 for this state is the question. In an insulin resistant state, the level of FI can

712 increase by about 10-fold the normal. However, the difference between the lower

713 and upper limit of glucose in a pre-diabetic state is less than 1.5-fold. To achieve a

714 tenfold increase in the effect resulting from a 1.5 fold increase in the causal

715 variable, the slope needs to be of the order of 7 to 8. However in the data, the

716 regression slope ranges between 0.05 and 0.2 (Table 11). Therefore the variance in

717 FI is unlikely to be caused by variance in glucose following insulin resistance.

44

718　　　　　　Therefore, we need to conclude that most of the variation in FI appears to be

719　　　　　　random error independent of insulin resistance.

720

721　**Table 11. Testing the putative pathway leading to a hyperinsulinemic, normoglycemic,**

722　**insulin resistant prediabetic state.**

723　**a.　Fasting glucose and fasting insulin in the four datasets**

Data source	FG mean (s.d.)	FI mean (s.d.)
CRISIS (n=558)	94 (18.70)	7.58 (1.82)
KEM (n=299)	86.35 (11.21)	11.84 (10.82)
NHP-SA (n=413)	98.86 (7.37)	11.11 (9.26)
NHP-EU (n=595)	99.90 (6.40)	8.41 (5.29)

724

725　**b. Correlations between FG, FI, HOMA-IR and HOMA beta in the four data sets**

726

727
728
729

	FG:FI		FG:HOMA IR		FG:HOMA beta		FI:HOMA IR		FI:HOMA beta		HOMA IR:HOMA beta	
	r(M)	ρ	r	ρ	r	ρ	r	ρ	r	ρ	r	ρ
CRISIS (n=558)	0.217 (0.055)	0.284	0.525	0.465	-0.209	-0.403	0.931	0.975	0.232	0.698	0.312	0.543
KEM (n=299)	0.198 (0.191)	0.241	0.317	0.352	-0.219	-0.259	0.985	0.990	0.532	0.811	0.633	0.746
NHP-SA (n=413)	0.163 (0.206)	0.282	0.236	0.464	-0.198	-0.145	0.995	0.990	0.763	0.875	0.833	0.810
NHP-EU (n=595)	0.223 (0.185)	0.261	0.309	0.464	-0.064	-0.055	0.994	0.993	0.891	0.933	0.904	0.886

730　**c.　C**

731　**onv**

732　**erg**

733　**ent**

734　**pat**

735　**hw**

736   **ay (A=Glucose, B=HOMA IR, C=Insulin)**

737

Prediction R1 r^2AC $<r^2AB.r^2BC$		CI of r^2AC		CI of $r^2AB.r^2BC$		Accepted/Rejected
		Lower	**Upper**	**Lower**	**Upper**	
	CRISIS	0.013	0.081	0.180	0.300	Accepted
	KEM	-0.004	0.082	0.035	0.162	Not rejected
	NHP-SA	-0.004	0.057	0.013	0.098	Not rejected
	NHP-EU	0.016	0.084	0.050	0.139	Not rejected
Prediction R2 **Mca<Mba.Mcb**		CI of Mca		CI of Mba.Mcb		Accepted/Rejected
		Lower	**Upper**	**Lower**	**Upper**	
	CRISIS	-0.053	0.163	0.104	0.146	Accepted
	KEM	-0.185	0.568	0.195	0.413	Accepted
	NHP-SA	-0.199	0.611	0.1761	0.418	Accepted
	NHP-EU	-0.178	0.548	0.190	0.320	Accepted

Prediction R3 rEbaEcb>0		CI of rEbaEcb			Accepted/Rejected
		Lower	**Upper**		
	CRISIS	0.390	0.521		Accepted
	KEM	0.118	0.333		Accepted
	NHP-SA	0.081	0.268		Accepted
	NHP-EU	0.178	0.328		Accepted

Prediction 4a rEbaC>rBC		CI rEbaC		CI rBC		Accepted/Rejected
		Lower	**Upper**	**Lower**	**Upper**	
	CRISIS	0.953	0.965	0.918	0.941	Accepted
	KEM	0.966	0.978	0.982	0.988	Rejected
	NHP-SA	0.980961	0.987	0.994	0.995	Rejected
	NHP-EU	0.968	0.977	0.993	0.995	Rejected

738

739   d. **Negative feedback pathway (A= HOMA IR, B=Glucose, C=Insulin)**

Prediction R1 r^2AC $>r^2AB.r^2BC$		CI r^2AC		CI of $r^2AB.r^2BC$		Accepted/Rejected
		Lower	Upper	Lower	Upper	
	CRISIS	0.845	0.886	0.003	0.300	Accepted
	KEM	0.9652	0.978	-0.001	0.161	Accepted
	NHP-SA	0.988	0.99	-4.8695E-05	0.006	Accepted
	NHP-EU	0.986	0.990	0.001	0.012	Accepted
Prediction R2 Mca>Mba.Mcb		CI Mca		CI of Mba.Mcb		Accepted/Rejected
		Lower	Upper	Lower	Upper	
	CRISIS	-3.242	9.967	0.222	0.641	Accepted
	KEM	0.083	0.299	0.080	0.587	Rejected
	NHP-SA	0.085	0.326	0.038	0.334	Accepted
	NHP-EU	-3.766	11.581	0.132	0.457	Accepted
Prediction R3 rEbaEcb<0		Lower rEbaEcb		Upper rEbaEcb		Accepted/Rejected
	CRISIS	-0.574		-0.452		Accepted

	KEM	-0.414		-0.210		Accepted
	NHP-SA	-0.325		-0.142		Accepted
	NHP-EU	-0.379		-0.234		Accepted
Prediction R4a **rEbaC<rBC**		**CI rEbaC**		**CI rBC**		**Accepted/Rejected**
		Lower	**Upper**	**Lower**	**Upper**	
	CRISIS	-0.392	-0.243	0.136	0.294	Rejected
	KEM	-0.231	-0.008	0.087	0.305	Rejected
	NHP-SA	-0.168	0.023	0.068	0.256	Rejected
	NHP-EU	-0.167	-0.008	0.145	0.298	Rejected

740

741 Table 11 footnote: The classical pathway leading to a prediabetic state is tested using the

742 pathway prediction approach. (a) Means and standard deviations from the four data sets (b)

743 correlations obtained from empirical data (c) testing the four predictions for the null model (fig

744 5b) (d) testing the four predictions of a simplified classical negative feedback pathway (fig 5a).

745

746   (b) By the steady state equations, the slope of the regression of FI on FG should be

747   K_3/d. Empirical estimates for both K_3 and d are available (see S2 Text) and

748   therefore this prediction can be tested. The empirical estimates are $K_3 = 0.08$

749   microIU.mg/min and $d = 0.15$/min respectively, and thereby the expected slope is

750   0.533. In all the four data sets, the slopes are significantly smaller than the ones

751   predicted from the empirical estimates (0.05 to 0.2). Thus, apart from a mismatch

752   between the slope required to cause the observed variation in FI and actual slopes,

753   the slopes expected from the empirical estimates of parameters and those obtained

754   in regression also do not match. The latter mismatch by itself may not be sufficient

755   to reject the pathway since a large measurement error in the X variable, i.e. FG can

756   lead to underestimation of regression slope, but this explanation implies that a

757   substantial part of variation in glucose is independent of insulin resistance, and is

758   akin to random error with respect to the hypothetical causal pathway.

759   (c) HOMA-β in our assumption represents K_3. However K_3 is a constant in our model,

760   and although it may have some variability in the population, it is uncorrelated with

761   the three variables of concern. Therefore, HOMA-β should show no significant

762   correlation with FG, FI and HOMA-IR. However, in all the four data sets HOMA-

763   β is significantly positively correlated with FI, but negatively correlated with FG

764   and positively correlated with HOMA-IR.

765   (d) In a negative feedback pathway $r_{AC}^2 > r_{AB}^2 . r_{BC}^2$. Qualitatively this inequality is true

766   for HOMA-IR, FG and FI in the data. However, simulations show that there is

767   overfitting of the inequality. r_{AC}^2 in all the four sets of data are substantially higher

768   than the distribution obtained in the simulations (Fig 6). The correlation between

769   FI and HOMA-IR is far greater than that predicted by the simulations, leading to

770   an overfitting rejection.

771   Thus if we assume the two HOMA indices to faithfully represent insulin resistance

772   and beta cell response respectively, then classical pathway needs to be rejected

773   owing to mismatches with many of its predictions.

774

775   **Fig 6:** Frequency distribution of correlation coefficients in simulations of the classical pathway

776   leading to prediabetic state: Bars represent the distribution of Pearson's correlations obtained in

777   10000 runs of simulations. The arrows indicate Pearson's correlations in the four sets of

778   empirical data. The distribution generated by simulations matches well with the real life

779   correlations for true IR-FG (grey bars and arrows), FG-FI (red bars and arrows), and the product

780   of the two (purple bars and arrows). The correlation between true IR and FI is greater than the

781   product as predicted by the pathway (green bars, we do not have empirical estimates of these

782   correlations) but the correlation between HOMA-IR and FI (blue bars and arrows) is

783   substantially greater than the predicted leading to an overfitting rejection. This indicates that

784   either HOMA-IR as currently calculated is substantially different from true insulin resistance or

785   the pathway get rejected based on this prediction.

786

787   e. Effects of deriving HOMA-IR and HOMA-β from FG and FI: Since HOMA-

788   IR and HOMA-β are not independently measured but derived from FG and FI

789   measurements, some correlations will follow from the derivations themselves.

790   The overfitting anomaly observed above can be explained as an artifact

791   coming out of the calculation of HOMA-IR. However, some other anomalies

792   remain unexplained. Here we are assuming that the classical pathway is true

793   and therefore, FI is a linear function of FG. If FI is represented as $m.FG + e$,

794   HOMA-IR will be correlated to FG^2. Similarly, HOMA-β should be

795   represented as $m.FG/(FG – 63)+e$. Under normal physiological range, FG >

796   63 and therefore HOMA-β is a decreasing function of FG. As a result both FI

797   and HOMA-IR should be negatively correlated to HOMA-β. Simulations of

798   the pathway results in a negative correlation between HOMA-IR and HOMA-

799   β as long as the errors are small to moderate. These expectations do not match

800   the empirical data, in which FI and HOMA-IR have significant positive

801   correlations with HOMA-β. Thus, accepting the classical pathway with some

802   allowance for artifacts coming out of the derived variables is not sufficient to

803   explain the empirical correlations.

804   f.   Testing the predictions of the null model: If FG and FI are independent of

805   each other and have some variance around a mean, HOMA-IR is expected to

806   be positively correlated with both since it is a product of the two. FI should be

807   positively correlated with HOMA-β, but FG should be negatively correlated

808   with HOMA-β. In the HOMA-IR- HOMA-β relationship, FI is in the

809   numerator of both. FG is in the numerator of HOMA-IR but in the

810   denominator of HOMA-β. Nevertheless, since the coefficient of variation of

811   FI is substantially greater than that of FG, FI is expected to dominate the

812   relationship and result in a positive correlation between HOMA-IR and

813   HOMA- β. All these predictions are observed in the data. The mismatch of the

814   null model with the data is that it assumes FG and FI to be independent and

815   uncorrelated. In all the four sets of data, there is a significant but weak

816   correlation between the two. The r^2 ranges from 0.026 to 0.049, and thus not

817   more than 5 % of variance is explained by the relationship.

818   If we consider FG and FI to be independent and HOMA-IR and HOMA-β derived

819   from them, they constitute a convergent pathway that can be tested by the pathway

820   predictions. It can be seen that predictions from R1, R2 and R3 of the convergent

821   pathway are accepted. However, prediction from R4 and the pathway-specific

822   prediction are rejected (Table 11b). These rejections can be explained by the positive

823   correlation between FG and FI. We have seen in the analysis of pathway P3 that if A

824   and C are positively correlated then $r^2_{AB} + r^2_{BC}$ can be greater than 1. The rejection of

825   the null model suggests that there is a relationship between FG and FI, but does not

826   indicate whether it comes from the classical pathway or through any other source as in

827   Fig 5c.

828

829   g. If we ignore the non-linearity of the model and assume HOMA-IR and

830   HOMA-β to faithfully represent insulin resistance and beta cell response, we

831   may use the 4 predictions of the standard negative feedback pathway. It is

832   seen that predictions from R1, R2 and R3 are accepted but the outcome of

833   prediction from R4 is complex (Table 11c). After correcting for the effect of

834   HOMA-IR, the FG-FI correlation should be weakened and that difference

835   would be predicted by the correlation between HOMA-IR and FG. However

836   instead of weakening, the FG-FI correlation becomes negative. Because of the

837   strong positive correlation between HOMA-IR and FI, correcting for HOMA-

838   IR subtracts from every value of FG, a quantity proportionate to FI, leading to

839   a negative correlation between the corrected FG and FI. Additionally,

840   simulations of the pathway show that if true insulin resistance is assumed to

841   be correlated to FG by the same order as HOMA-IR, the correlation of true

842   insulin resistance with FI is far less than that between HOMA-IR and FI (a

843   result similar to Fig 6 and therefore not separately shown). Thus, there is an

844   overfitting rejection of prediction from R1 as well. Rejection of this pathway

845   based on two predictions is due to the unrealistically strong correlation

846   between HOMA-IR and FI, which comes from the calculation of HOMA-IR

847   itself.

848

849   We need to examine now to what extent HOMA-IR faithfully represents the true insulin

850   resistance because if it does, the classical pathway certainly gets rejected. This can be examined

851   in the simulations since the true insulin resistance is an input variable and HOMA-IR can be

852   calculated as an outcome of the simulations. We see that HOMA-IR is correlated well with true

853   insulin resistance when both e_1 and e_2 are close to zero (Fig 7). As the errors increase, the

854   correlation becomes weaker. In the data, we do not have access to e_1 and e_2 but since the FG-FI

855   correlation also becomes weaker with e_2, we can look at how HOMA-IR represents true insulin

856   resistance at different levels of FG-FI correlation. It can be seen that as FG-FI correlation

857   becomes weak, HOMA-IR correlation with the true insulin resistance also becomes weak (Fig

858   7), but this relationship is affected by e_1. When e_1 is close to zero, i.e. almost all the variation in

859   FG is explained by variation in true insulin resistance, even at low FG-FI correlation, HOMA-IR

860   represents true insulin resistance fairly well, their correlation ranging between 0.58 and 0.7. On

861   the other hand if we assume e_1 to be large i.e. most of the variation in FG is due to random error

862   or effects independent of insulin action, HOMA-IR is poorly correlated with true insulin

863   resistance, the correlation coefficient declining to 0.2. Thus if we assume that the variance in FG

864   is mainly caused by insulin resistance, then we have to reject the classical pathway leading to

865   hyperinsulinemia. Alternatively, it is likely that the classical pathway is true but HOMA-IR does

866   not represent true insulin resistance and that most of the variation in FG is not caused by insulin

867   resistance. The substantially lower than expected slope of the FG-FI regression suggests large

868   random errors in FG making the second interpretation more likely. In any case the classical

869   pathway and the faithfulness of HOMA indices cannot be simultaneously true, and we have to

870   reject at least one of them.

871   Results of the four alternative approaches to analyze the classical pathway and the null model

872   converge on the inference that the null model is rejected on the basis of a weak but significant

873   correlation between FG and FI. But the weak correlation in FG and FI is not adequately

874   explained by the classical pathway owing to multiple mismatches and rejection of many of its

875   predictions. The pathway rejection may be partially saved by saying that HOMA-IR and HOMA-

876   β are not good indicators of insulin resistance and beta cell response and that we do not have

877   access to true insulin reistance to test the predictions. However the FG-FI regression slope also

878   has a large mismatch with expectations derived from the variance in FI as well as from empirical

879   estimates of K_3 and d. Therefore, it seems more likely that FG and FI are related by causes other

880   than the classical pathway, and HOMA-IR and HOMA- β are derived artificial constructs that do

881   not represent any real life phenomena.

882   There are a number of real life interpretations of the pathway in Fig 5c. Autonomic inputs from

883   the nervous system are known to affect both insulin secretion and liver glucose production,

884 which might be represented by the common cause arrows of Fig 5c. Alternatively, a small error

885 in data collection can also result in the observed FG-FI correlation. The fasting sampling is done

886 by instructing the subjects to have no food or drink after the last evening meal. However, if even

887 a small proportion of subjects happen to consume bed tea an hour or two before sampling, their

888 glucose as well as insulin levels could be slightly elevated simultaneously. This can result in a

889 weak positive correlation between FG and FI in the data. Since the fasting state is based on the

890 honesty of the subjects and there is no independent monitoring, this source of error cannot be

891 ignored. Thus, there are more than one possible reasons for external factors causing a weak

892 correlation between FG and FI, and the correlation is not sufficient to support the classical

893 pathway in the presence of multiple other mismatches.

894

895 **Fig 7**: The reliability of HOMA-IR as an index of true insulin resistance: The pathway

896 simulations were carried out at a standard deviation of e_1=1 (blue dots) and 10 (red dots). The

897 FG-FI correlation weakens with increase in e_2 which also affects the correlation between true IR

898 and HOMA-IR. It can be seen that HOMA-IR is a reliable indicator of insulin resistance when e_1

899 is small, but at large e_1 it is a poor indicator as suggested by a weak correlation with true insulin

900 resistance.

901

902 It should be noted that the correlational patterns in the four data sets used are remarkably similar

903 although they come from populations differing in location, ethnicity and culture. It would be

904 important to see whether the same correlational patterns are observed in other populations as

905 well, but we can be confident in rejecting the classical pathway at least in the populations

906 sampled.

907

What can type 2 diabetes research gain from our analysis

Putting the results together, it can safely be concluded that HOMA-IR and HOMA-β appear to be artificial constructs and reflect very marginally, if at all, the true insulin resistance and β cell response in a steady state. Until our approach for testing a causal pathway was available, there was no way to test whether HOMA-IR and HOMA-β truly represent the intended states of the system. Because of this limitation, insulin resistance was a circular argument. The inability of insulin to regulate glucose was assumed to be because of insulin resistance, but insulin resistance was measured as the inability of insulin to regulate glucose. This circularity had made the hypothesis of insulin resistance and compensatory hyperinsulinemia non-falsifiable. Our approach to pathway predictions breaks the circularity, and makes it possible to test whether the insulin resistance and glucose-mediated compensatory hyperinsulinemia hypothesis is supported by epidemiological data. At least in the populations tested, many serious anomalies in the classical pathway leading to a hyperinsulinemic, normoglycemic, insulin resistance prediabetic state are exposed. Conservatively we can argue that since HOMA-IR and HOMA-β do not represent insulin resistance and β cell response faithfully, and we do not have alternative measures for them, it may not be possible to clearly reject the classical pathway, but the data clearly show that even if true, the classical pathway has a very limited role in deciding FG, FI and their inter-relationship. Both the steady state levels have a large component of error or effects independent of the pathway under consideration. Although our analysis is restricted to the prediabetic state at present, establishing causality in the prediabetic state has implications for the over diabetic state. According to classical thinking, a failure of compensatory insulin response leads to diabetic hyperglycemia. Since our analysis questions the compensatory insulin response

57

930   itself, the pathway leading to hyperglycemia is also in question. Even a highly conservative

931   inference would demand rethinking of the causal process leading to diabetes.

932   Doubts about the classical pathway are raised independently by experiments using insulin

933   receptor knockouts or insulin suppression. Muscle-specific insulin receptor knockouts show

934   altered glucose tolerance curves but normal fasting insulin (42). Insulin suppression experiments

935   do not result in elevated fasting glucose (43–45). Inactivation of insulin degrading enzyme raises

936   steady state insulin levels but does not decrease glucose levels (46,47). These experiments have

937   already challenged the classical pathway. Thus, there are multiple reasons to doubt the classical

938   pathway. On the other hand, a number of factors other than the mutual effects of FG and FI are

939   known to affect insulin response as well as glucose homeostasis (48–58), but these factors have

940   not been integrated into the mainstream glucose homeostasis models. We do not intend here to

941   test all possible alternative pathways deciding FG and FI. But our study lays down a set of

942   methods by which this can be done, once the pathway hypotheses are clearly spelt out and the

943   causal variables are measured. An important contribution of our methods is that physiological

944   causal pathways can be evaluated based on epidemiological data, which is potentially a very

945   important tool in understanding complex disorders. Experimental biology reveals what *can*

946   happen in a system, but what *does* happen at the population level is better revealed by

947   epidemiological data. Therefore, discerning causal signatures of pathophysiological pathways in

948   epidemiological data is likely to be an important breakthrough.

949

Conclusions

Making causal inferences from cross sectional correlational data is a long-standing problem. A correlation between two variables does not give reliable information about causal relations. However, we demonstrate here, in the context of steady state homeostatic systems, using mathematical proofs as well as simulations from causal pathways that, in a set of three or more correlated variables, it is possible to test causal hypotheses based on the interrelationships of regression-correlation parameters. This is potentially a highly valuable tool in making causal inferences from cross sectional data in several fields.

Using this set of principles, we tested the classical causal assumption behind the hyperinsulinemic, normoglycemic, insulin resistant or pre-diabetic state. The analysis showed that this causal pathway and the measures of insulin resistance and insulin response were not supported by epidemiological data. Thus, the objections raised recently to the classical causal pathway are validated and alternative causal pathways that already have substantial experimental evidence need to be integrated in the mainstream clinical thinking.

Acknowledgements

965

966 We thank Chittaranjan Yajnik for making the CRISIS and PMNS data sets available to us. We

967 would also like to thank Louise Hayes and Raj Bhopal for making the data from NHP studies

968 available. We thank Subhash Lele and Anil Gore for useful comments on an earlier draft

969 manuscript. We also thank Rajiv Gandhi Science and Technology Commission, (RGSTC),

970 Maharashtra State, India for partial support.

971

References

972

973   1.   Baker JP. Mercury, Vaccines, and Autism. Am J Public Health [Internet]. 2008

974   Feb;98(2):244–53. Available from:

975   http://ajph.aphapublications.org/doi/10.2105/AJPH.2007.113159

976   2.   DeStefano F. Vaccines and Autism: Evidence Does Not Support a Causal Association.

977   Clin Pharmacol Ther [Internet]. 2007 Dec 10;82(6):756–9. Available from:

978   http://doi.wiley.com/10.1038/sj.clpt.6100407

979   3.   Parascandola M, Weed DL. Causation in epidemiology. J Epidemiol Community Health.

980   2001;55(12):905–12.

981   4.   Gerber JS, Offit PA. Vaccines and Autism: A Tale of Shifting Hypotheses. Clin Infect Dis

982   [Internet]. 2009 Feb 15;48(4):456–61. Available from:

983   https://academic.oup.com/cid/article-lookup/doi/10.1086/596476

984   5.   Ratzan SC. Setting the Record Straight: Vaccines, Autism, and the Lancet. J Health

985   Commun [Internet]. 2010 Apr 30;15(3):237–9. Available from:

986   http://www.tandfonline.com/doi/abs/10.1080/10810731003780714

987   6.   Ejima K, Li P, Smith DL, Nagy TR, Kadish I, van Groen T, et al. Observational research

988   rigour alone does not justify causal inference. Eur J Clin Invest [Internet]. 2016

989   Dec;46(12):985–93. Available from: http://doi.wiley.com/10.1111/eci.12681

990   7.   Hill AB. The Environment and Disease: Association or Causation? Proc R Soc Med. 1965

991   May;58(5):295–300.

992   8.   Meehl PE, Waller NG. The path analysis controversy: a new statistical approach to strong

993   appraisal of verisimilitude. Psychol Methods [Internet]. 2002 Sep;7(3):283–300. Available

994   from: http://www.ncbi.nlm.nih.gov/pubmed/12243300

995 9.   Niles HE. The Method of Path Coefficients an Answer to Wright. Genetics [Internet].

996   1923 May;8(3):256–60. Available from: http://www.ncbi.nlm.nih.gov/pubmed/17246012

997 10. Wright S. The Method of Path Coefficients. Ann Math Stat [Internet]. 1934 Sep;5(3):161–

998   215. Available from: http://projecteuclid.org/euclid.aoms/1177732676

999 11. Wright S. Path Coefficients and Path Regressions: Alternative or Complementary

1000   Concepts? Biometrics [Internet]. 1960 Jun;16(2):189. Available from:

1001   http://www.jstor.org/stable/2527551?origin=crossref

1002 12. Greenland S. An introduction to instrumental variables for epidemiologists. Int J

1003   Epidemiol [Internet]. 2000 Aug;29(4):722–9. Available from:

1004   https://academic.oup.com/ije/article-lookup/doi/10.1093/ije/29.4.722

1005 13. Granger CWJ. Investigating Causal Relations by Econometric Models and Cross-spectral

1006   Methods. Econometrica [Internet]. 1969 Aug;37(3):424. Available from:

1007   http://www.jstor.org/stable/1912791?origin=crossref

1008 14. Rosenbaum PR, Rubin DB. The central role of the propensity score in observational

1009   studies for causal effects. Biometrika [Internet]. 1983;70(1):41–55. Available from:

1010   https://academic.oup.com/biomet/article-lookup/doi/10.1093/biomet/70.1.41

1011 15. Peters J, Janzing D, Scholkopf B. Causal Inference on Discrete Data Using Additive Noise

1012   Models. IEEE Trans Pattern Anal Mach Intell. 2011 Dec;33(12):2436–50.

1013 16. Neuberg LG. CAUSALITY: MODELS, REASONING, AND INFERENCE, by Judea

1014   Pearl, Cambridge University Press, 2000. Econom Theory [Internet]. 2003 Aug 6;19(4).

1015   Available from: http://www.journals.cambridge.org/abstract_S0266466603004109

1016 17. Pearl J. Causal inference in statistics: An overview. Stat Surv [Internet]. 2009;3:96–146.

1017   Available from: http://projecteuclid.org/euclid.ssu/1255440554

1018   18.   Peters J, Janzing D, Scholkopf B. Causal Inference on Discrete Data Using Additive Noise

1019   Models. IEEE Trans Pattern Anal Mach Intell [Internet]. 2011 Dec;33(12):2436–50.

1020   Available from: http://ieeexplore.ieee.org/document/5740928/

1021   19.   Peters J, Mooij JM, Janzing D, Schölkopf B. Causal Discovery with Continuous Additive

1022   Noise Models. J Mach Learn Res. 2014;15:2009–53.

1023   20.   Eichler M. Causal inference with multiple time series: principles and problems. Philos

1024   Trans R Soc A Math Phys Eng Sci [Internet]. 2013 Jul 15;371(1997):20110613–

1025   20110613. Available from:

1026   http://rsta.royalsocietypublishing.org/cgi/doi/10.1098/rsta.2011.0613

1027   21.   Abdul-Ghani MA, Tripathy D, DeFronzo RA. Contributions of beta-cell dysfunction and

1028   insulin resistance to the pathogenesis of impaired glucose tolerance and impaired fasting

1029   glucose. Diabetes Care [Internet]. 2006 May;29(5):1130–9. Available from:

1030   http://www.ncbi.nlm.nih.gov/pubmed/16644654

1031   22.   Cerf ME. Beta Cell Dysfunction and Insulin Resistance. Front Endocrinol (Lausanne)

1032   [Internet]. 2013;4. Available from:

1033   http://journal.frontiersin.org/article/10.3389/fendo.2013.00037/abstract

1034   23.   Watve M. Doves, Diplomats, and Diabetes [Internet]. New York, NY: Springer New

1035   York; 2013. Available from: http://link.springer.com/10.1007/978-1-4614-4409-1

1036   24.   Dubuc PU. The development of obesity, hyperinsulinemia, and hyperglycemia in ob/ob

1037   mice. Metabolism [Internet]. 1976 Dec;25(12):1567–74. Available from:

1038   http://www.ncbi.nlm.nih.gov/pubmed/994838

1039   25.   Dubuc PU. Non-essential role of dietary factors in the development of diabetes in ob/ob

1040   mice. J Nutr [Internet]. 1981 Oct;111(10):1742–8. Available from:

1041   http://www.ncbi.nlm.nih.gov/pubmed/7026742

1042   26.   Garvey WT, Olefsky JM, Marshall S. Insulin induces progressive insulin resistance in

1043   cultured rat adipocytes. Sequential effects at receptor and multiple postreceptor sites.

1044   Diabetes [Internet]. 1986 Mar;35(3):258–67. Available from:

1045   http://www.ncbi.nlm.nih.gov/pubmed/3512337

1046   27.   Shanik MH, Xu Y, Skrha J, Dankner R, Zick Y, Roth J. Insulin Resistance and

1047   Hyperinsulinemia: Is hyperinsulinemia the cart or the horse? Diabetes Care [Internet].

1048   2008 Feb 1;31(Supplement 2):S262–8. Available from:

1049   http://care.diabetesjournals.org/cgi/doi/10.2337/dc08-s264

1050   28.   Corkey BE. Banting lecture 2011: hyperinsulinemia: cause or consequence? Diabetes

1051   [Internet]. 2012 Jan;61(1):4–13. Available from:

1052   http://www.ncbi.nlm.nih.gov/pubmed/22187369

1053   29.   Lerner RL, Porte D. Acute and steady-state insulin responses to glucose in nonobese

1054   diabetic subjects. J Clin Invest [Internet]. 1972 Jul 1;51(7):1624–31. Available from:

1055   http://www.jci.org/articles/view/106963

1056   30.   Turner RC, Holman RR, Matthews D, Hockaday TD, Peto J. Insulin deficiency and

1057   insulin resistance interaction in diabetes: estimation of their relative contribution by

1058   feedback analysis from basal plasma insulin and glucose concentrations. Metabolism

1059   [Internet]. 1979 Nov;28(11):1086–96. Available from:

1060   http://www.ncbi.nlm.nih.gov/pubmed/386029

1061   31.   Halter JB, Ward WK, Porte D, Best JD, Pfeifer MA. Glucose regulation in non-insulin-

1062   dependent diabetes mellitus. Interaction between pancreatic islets and the liver. Am J Med

1063   [Internet]. 1985 Aug 23;79(2B):6–12. Available from:

1064   http://www.ncbi.nlm.nih.gov/pubmed/2863979

1065 32. Matthews DR, Hosker JP, Rudenski AS, Naylor BA, Treacher DF, Turner RC.

1066   Homeostasis model assessment: insulin resistance and□?-cell function from fasting

1067   plasma glucose and insulin concentrations in man. Diabetologia [Internet]. 1985

1068   Jul;28(7):412–9. Available from: http://link.springer.com/10.1007/BF00280883

1069 33. Fuller WA, editor. Measurement Error Models [Internet]. Hoboken, NJ, USA: John Wiley

1070   & Sons, Inc.; 1987. (Wiley Series in Probability and Statistics). Available from:

1071   http://doi.wiley.com/10.1002/9780470316665

1072 34. Griggs RC, Kingston W, Jozefowicz RF, Herr BE, Forbes G, Halliday D. Effect of

1073   testosterone on muscle mass and muscle protein synthesis. J Appl Physiol [Internet]. 1989

1074   Jan;66(1):498–503. Available from: http://www.ncbi.nlm.nih.gov/pubmed/2917954

1075 35. Kraemer WJ, Ratamess NA. Hormonal responses and adaptations to resistance exercise

1076   and training. Sports Med [Internet]. 2005;35(4):339–61. Available from:

1077   http://www.ncbi.nlm.nih.gov/pubmed/15831061

1078 36. Cumming DC, Brunsting LA, Strich G, Ries AL, Rebar RW. Reproductive hormone

1079   increases in response to acute exercise in men. Med Sci Sports Exerc [Internet]. 1986

1080   Aug;18(4):369–73. Available from: http://www.ncbi.nlm.nih.gov/pubmed/2943968

1081 37. Tomasi T, Sledz D, Wales JK, Recant L. Insulin half-life in normal and diabetic subjects.

1082   Rev Neuropsychiatr Infant [Internet]. 1966 Dec;14(12):315–7. Available from:

1083   http://www.ncbi.nlm.nih.gov/pubmed/5988016

1084 38. Pories WJ, Dohm GL. Diabetes: Have We Got It All Wrong?: Hyperinsulinism as the

1085   culprit: surgery provides the evidence. Diabetes Care [Internet]. 2012 Dec 1;35(12):2438–

1086   42. Available from: http://care.diabetesjournals.org/cgi/doi/10.2337/dc12-0684

1087 39. Yajnik CS, Joglekar C V, Lubree HG, Rege SS, Naik SS, Bhat DS, et al. Adiposity,

1088   inflammation and hyperglycaemia in rural and urban Indian men: Coronary Risk of

1089   Insulin Sensitivity in Indian Subjects (CRISIS) Study. Diabetologia [Internet]. 2008

1090   Jan;51(1):39–46. Available from: http://www.ncbi.nlm.nih.gov/pubmed/17972060

1091 40. Bhopal R, Unwin N, White M, Yallop J, Walker L, Alberti KGMM, et al. Heterogeneity

1092   of coronary heart disease risk factors in Indian, Pakistani, Bangladeshi, and European

1093   origin populations: cross sectional study. BMJ [Internet]. 1999 Jul 24;319(7204):215–20.

1094   Available from: http://www.bmj.com/cgi/doi/10.1136/bmj.319.7204.215

1095 41. Joshi NP, Kulkarni SR, Yajnik CS, Joglekar C V., Rao S, Coyaji KJ, et al. Increasing

1096   maternal parity predicts neonatal adiposity: Pune Maternal Nutrition Study. Am J Obstet

1097   Gynecol. 2005;193(3):783–9.

1098 42. Kadowaki T. Insights into insulin resistance and type 2 diabetes from knockout mouse

1099   models. J Clin Invest [Internet]. 2000 Aug 15;106(4):459–65. Available from:

1100   http://www.jci.org/articles/view/10830

1101 43. Gill G V., Rauf O, MacFarlane IA. Diazoxide treatment for insulinoma: a national UK

1102   survey. Postgrad Med J [Internet]. 1997 Oct 1;73(864):640–1. Available from:

1103   http://pmj.bmj.com/cgi/doi/10.1136/pgmj.73.864.640

1104 44. Alemzadeh R, Karlstad MD, Tushaus K, Buchholz M. Diazoxide enhances basal

1105   metabolic rate and fat oxidation in obese Zucker rats. Metabolism [Internet]. 2008

1106   Nov;57(11):1597–607. Available from:

1107   http://linkinghub.elsevier.com/retrieve/pii/S0026049508002382

1108 45. Alemzadeh R, Tushaus KM. Modulation of Adipoinsular Axis in Prediabetic Zucker

1109   Diabetic Fatty Rats by Diazoxide. Endocrinology [Internet]. 2004 Dec;145(12):5476–84.

1110   Available from: https://academic.oup.com/endo/article-lookup/doi/10.1210/en.2003-1523

1111 46. Maianti JP, McFedries A, Foda ZH, Kleiner RE, Du XQ, Leissring MA, et al. Anti-

1112   diabetic activity of insulin-degrading enzyme inhibitors mediated by multiple hormones.

1113   Nature [Internet]. 2014 Jul 21;511(7507):94–8. Available from:

1114   http://www.nature.com/articles/nature13297

1115 47. Abdul-Hay SO, Kang D, McBride M, Li L, Zhao J, Leissring MA. Deletion of insulin-

1116   degrading enzyme elicits antipodal, age-dependent effects on glucose and insulin

1117   tolerance. PLoS One [Internet]. 2011;6(6):e20818. Available from:

1118   http://www.ncbi.nlm.nih.gov/pubmed/21695259

1119 48. Levinger I, Goodman C, Matthews V, Hare DL, Jerums G, Garnham A, et al. BDNF,

1120   Metabolic Risk Factors, and Resistance Training in Middle-Aged Individuals. Med Sci

1121   Sport Exerc [Internet]. 2008 Mar;40(3):535–41. Available from:

1122   https://insights.ovid.com/crossref?an=00005768-200803000-00020

1123 49. Reinehr T, Roth CL. A new link between skeleton, obesity and insulin resistance:

1124   relationships between osteocalcin, leptin and insulin resistance in obese children before

1125   and after weight loss. Int J Obes [Internet]. 2010 May 12;34(5):852–8. Available from:

1126   http://www.nature.com/articles/ijo2009282

1127 50. Polgreen LE, Jacobs DR, Nathan BM, Steinberger J, Moran A, Sinaiko AR. Association

1128   of Osteocalcin With Obesity, Insulin Resistance, and Cardiovascular Risk Factors in

1129   Young Adults. Obesity [Internet]. 2012 Nov;20(11):2194–201. Available from:

1130   http://doi.wiley.com/10.1038/oby.2012.108

1131 51. Lo C-M, Obici S, Dong HH, Haas M, Lou D, Kim DH, et al. Impaired insulin secretion

1132   and enhanced insulin sensitivity in cholecystokinin-deficient mice. Diabetes [Internet].

1133   2011 Jul;60(7):2000–7. Available from: http://www.ncbi.nlm.nih.gov/pubmed/21602512

1134 52. Han DH, Hansen PA, Chen MM, Holloszy JO. DHEA treatment reduces fat accumulation

1135   and protects against insulin resistance in male rats. J Gerontol A Biol Sci Med Sci

1136   [Internet]. 1998 Jan;53(1):B19-24. Available from:

1137   http://www.ncbi.nlm.nih.gov/pubmed/9467418

1138 53. Pitteloud N, Mootha VK, Dwyer AA, Hardin M, Lee H, Eriksson K-F, et al. Relationship

1139   between testosterone levels, insulin sensitivity, and mitochondrial function in men.

1140   Diabetes Care [Internet]. 2005 Jul;28(7):1636–42. Available from:

1141   http://www.ncbi.nlm.nih.gov/pubmed/15983313

1142 54. Polderman KH, Gooren LJ, Asscheman H, Bakker A, Heine RJ. Induction of insulin

1143   resistance by androgens and estrogens. J Clin Endocrinol Metab [Internet]. 1994

1144   Jul;79(1):265–71. Available from: http://www.ncbi.nlm.nih.gov/pubmed/8027240

1145 55. Nonogaki K. New insights into sympathetic regulation of glucose and fat metabolism.

1146   Diabetologia [Internet]. 2000 May;43(5):533–49. Available from:

1147   http://www.ncbi.nlm.nih.gov/pubmed/10855527

1148 56. Meek TH, Wisse BE, Thaler JP, Guyenet SJ, Matsen ME, Fischer JD, et al. BDNF action

1149   in the brain attenuates diabetic hyperglycemia via insulin-independent inhibition of

1150   hepatic glucose production. Diabetes [Internet]. 2013 May;62(5):1512–8. Available from:

1151   http://www.ncbi.nlm.nih.gov/pubmed/23274899

1152 57. Holmaeng A, Bjoerntorp P. The effects of testosterone on insulin sensitivity in male rats.

1153   Acta Physiol Scand [Internet]. 1992 Dec;146(4):505–10. Available from:

1154   http://doi.wiley.com/10.1111/j.1748-1716.1992.tb09452.x

1155 58. Parton LE, Ye CP, Coppari R, Enriori PJ, Choi B, Zhang C-Y, et al. Glucose sensing by

1156   POMC neurons regulates glucose homeostasis and is impaired in obesity. Nature

1157   [Internet]. 2007 Sep 29;449(7159):228–32. Available from:

1158   http://www.nature.com/articles/nature06098

1159

1160

Supporting Information

1161

1162 **S1 Text.** Deriving predictions for regression parameters based on causal equations and

1163 calculation of causal parameters for simulations.

1164

1165 **S2 Text.** Empirical estimates for parameters used in simulations.

Acyclic pathways

P1: Linear
A → B → C

P2: Radiating
A ← B → C

P3: Convergent
A → B ← C
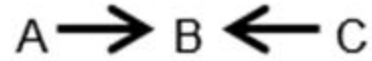
P4: Common cause
X
↙ ↓ ↘
A   B   C
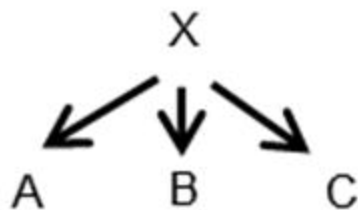
P5a: Single different cause
X
↙ ↓
A → B   C
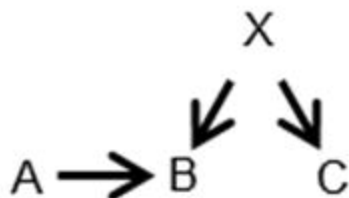
P5b: Double different causes
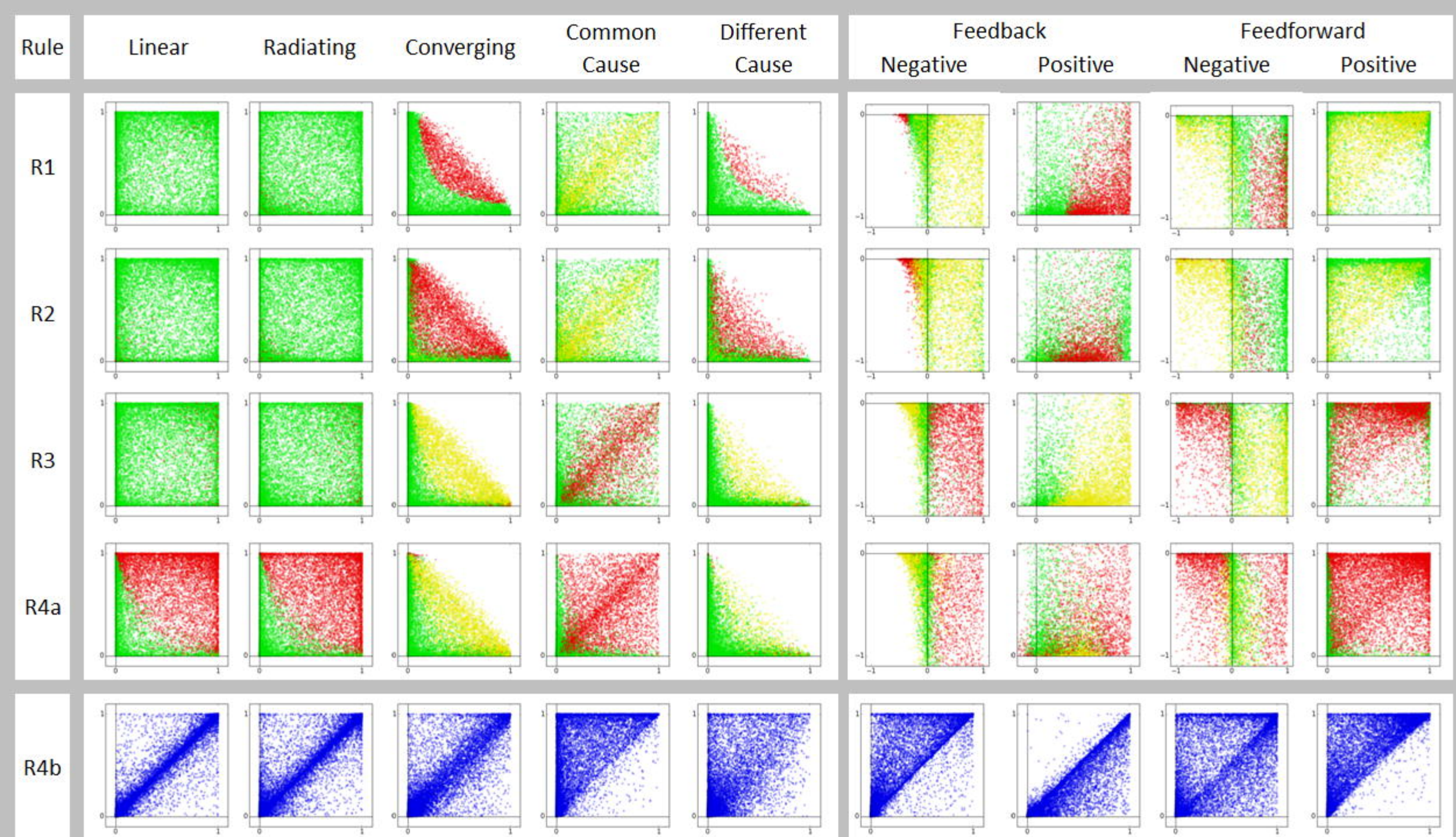X   Y
↙ ↓ ↓ ↓
A   B   C
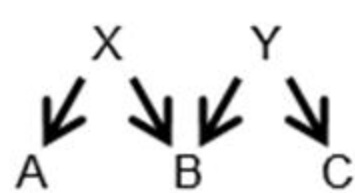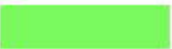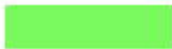
Cyclic pathways

P6: Positive or negative feedback
A → B → C
A → B → C
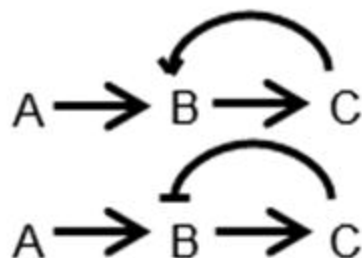
P7: Positive or negative feedforward
A → B → C
A → B → C
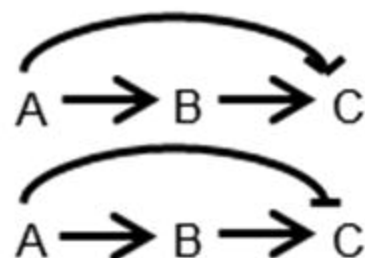
Rule	Linear	Radiating	Converging	Common Cause	Different Cause	Feedback		Feedforward	
						-	+	-	+
R1	green	green	red	yellow	red	yellow	red	red	yellow
R2	green	green	red	yellow	red	yellow	red	red	yellow
R3	green	green	yellow	red	yellow	red	yellow	red	red
R4a	red	red	yellow	red	yellow	red	red*	red**	red
R4b	green	green	green	yellow	green	yellow	red	red/green/yellow	yellow

Rule	Linear	Radiating	Converging	Common Cause	Different Cause	Feedback Negative	Feedback Positive	Feedforward Negative	Feedforward Positive
R1									
R2									
R3									
R4a									
R4b									

Sample Size	N = 100	N=500
Converging, R1		
Different Cause, R4b		
Feedforward -ve, R2		
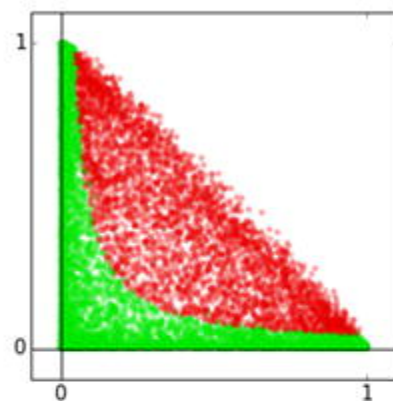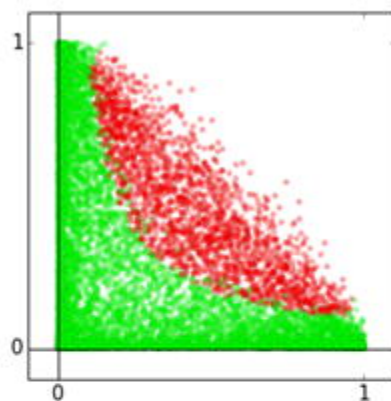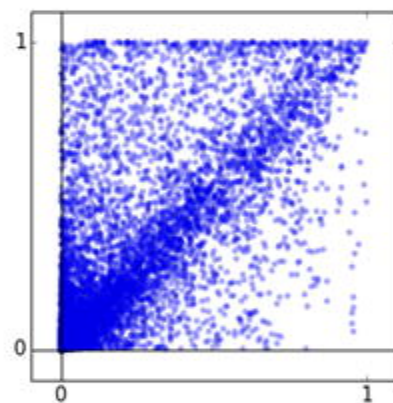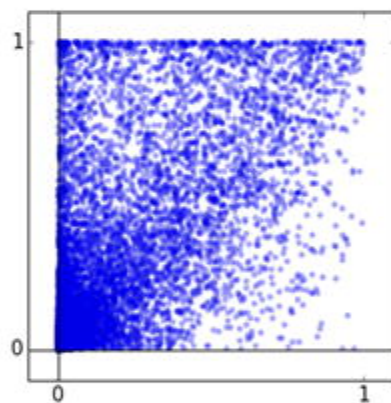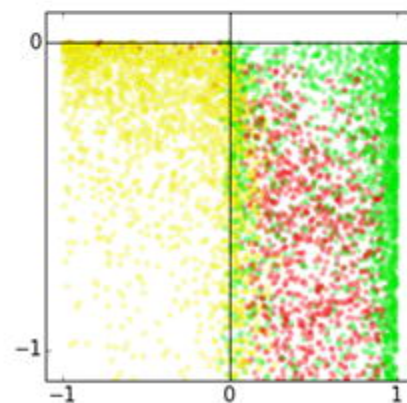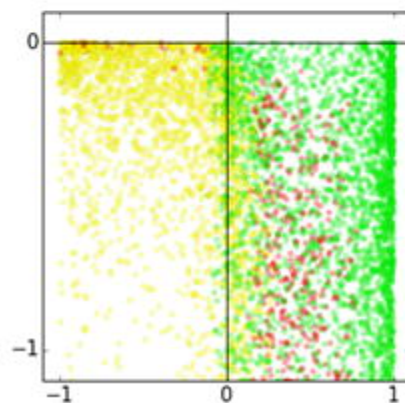
a.   IR (HOMA IR) → Glucose → Insulin

b.   Glucose → HOMA IR ← Insulin

X

c.   Glucose → HOMA IR ← Insulin

IR (HOMA IR)

d.   Liver ⫞⟹ Glucose → Insulin